TROUGH AND WRINKLING ANALYSIS OF NON-UNIFORM WEBS

By

AMOL MAHADEV PATIL

Bachelor of Science in Automobile Engineering

Shivaji University

Kolhapur, Maharashtra, India

2003

Submitted to the Faculty of the
Graduate College of the
Oklahoma State University
in partial fulfillment of
the requirements for
the Degree of
MASTER OF SCIENCE
May, 2010

TROUGH AND WRINKLING ANALYSIS OF NON-UNIFORM WEBS

Thesis Approved:

Dr. J. K. Good

Thesis Adviser

Dr. S. P. Harimkar

Dr. G. E. Young

Dr. A. Gordon Emslie

Dean of the Graduate College

ACKNOWLEDGMENTS

I would first like to express the deepest appreciation to my advisor, Dr. J. K. Good, who has the attitude and the substance of a genius: he continually and convincingly conveyed a spirit of adventure in regard to research, and an excitement in regard to teaching. Without his guidance and persistent help this thesis would not have been possible.

I would like to thank my committee members, Dr. S. P. Harimkar and Dr. G. E. Young for being on my committee. Their advice and assistance throughout the research was invaluable. I would like to extend my gratitude to Dr. Lu and Dr. Price who imparted great knowledge about materials and their applications and provided sound background in mechanics and stress analysis.

I would like to thank Ron Markum for his help during the research and the Sponsors of the WHRC for making this research possible. I would like to express sincere gratitude to my parents for their invaluable encouragement and to my fellow students for helping me during my research. Lastly, I offer my regards and blessings to all of those who supported me in any respect during the completion of the thesis.

Table 0f Contents

Chapter Page

List of Figures

Nomenclature

CMD	Cross Machine Direction
MD	Machine Direction
a	Span Length
A	Area of Cross-Section of the Web
As	Area of the Beam reacting shear
b	Total Web Width
b_1	Width of thicker section of the web
b_c	Distance of the Centroidal Axis from the Thinner side
Q	First Moment of Area at the Given Location
f_{yi}	Lateral force at the upstream roller
f_{yj}	Lateral force at the downstream roller
E	Young's Modulus
E_x, E_y	Directional Young's Modulus
G	Shear Modulus
h	Web Thickness
h_1	Thickness on the thinner side of the web
h_2	Thickness on the thicker side of the web
I	Web Area Moment of Inertia
M_i	Bending moment in web at upstream roller

M_j	Bending moment in web at downstream roller
R	Nominal Radius of Roller
T	Web Line Tension
FE	Finite Elements
V	Web Velocity
V_{avg}	Average web Velocity
ω	Angular velocity of the roller
x	Coordinate that aligns with the MD direction
y	Coordinate that aligns with the CMD direction
v	Poisson's Ratio
v_{xy}, v_{yx}	Directional Poisson's Ratio
ϕ	Shear Parameter
ε_{md}	Machine direction strain
γ_{xy}	Shear Strain
σ_{md}	Stress in machine direction
σ_x	Stress in x direction
σ_y	Stress in y direction
σ_{ycr}	Critical Lateral Normal Stress
m	Roller Taper
m_{cr}	Critical Roller Taper
θ_i	End rotation of web at upstream roller
θ_j	End rotation of web at downstream roller
v_i	Lateral deflection of web at upstream Roller
v_j	Lateral deflection of web at downstream Roller
τ	Shear Stress
τ_{max}	Maximum shear stress
τ_{cr}	Shear stress needed to induce troughs in the web

T_{slack}	Tension where Slack Edge Occurs
θ_{slack}	Misalignment where Slack Edge Occurs
m_{slack}	Taper where Slack Edge Occurs
k	Shear Stress Factor

CHAPTER I

Introduction

1.1 Wrinkling in Web Handling

A web is a long, thin and continuous sheet of material. The web material form can be advantageous when manufactured products can be made continuously instead of batch production. The web has a small in-plane bending stiffness (about the X and Y axes). There are a variety of materials in the market which can be classified as webs including papers, plastic films, foils, textiles products and composites. The lengths of webs are much greater than their widths and their widths are much greater than their thickness. Webs are transported through process machinery to enhance their value. Process operations can include coating, printing, slitting, laminating, folding and finally converting where the continuous form is cut to a discrete size and becomes a consumer product.

Web handling is the science associated with the transporting of a web through a web process machine. Process machines often first unwind a web and gain control of the lateral position of the web and the web tension. The web then transits several rollers and then enters one or more process operations. Depending on the length of the process machine and process needs the web may have to be guided into position and have the tension adjusted many times. Finally if all processing operations have been successful the web is rewound into a roll form for storage until it is needed in a subsequent processing machine. A single web may have to transit through many process machines before it is converted to a final product. This is typical because many processes have to occur at different speeds making it impossible for all process operations to occur within one process machine. As a result one web may undergo processing in several machines which raises the probability that manufacturing errors or flaws will occur. This thesis will focus upon web stability. Sometimes webs become unstable between and on rollers and interrupt the web process. Some of the reasons webs become unstable are known. They include roller misalignment, lateral motions of the web, diameter variations of rollers and wound rolls, negative bow of rollers which can be due to roller deformation resulting from web tension, decreases in web tension which results in web expansion, temperature effects, visco-elasticity or discontinuities in the web itself. Thus there are many reasons that an isotropic uniform web might become unstable.

Webs in process machines can be considered as a structure consisting series of plates and shells [18] as shown in Figure 1. While studying instability of webs their finite bending stiffness plays major role. Normally to transport a web through a machine

requires the web must be subjected to tension. This applied tension is responsible for forcing the web to conform to the shape of rollers in the form of a sector of a cylindrical shell. The rollers are supported on low friction bearings on their axis of symmetry. The tension in the web induces normal contact forces between the shells and the surface of rollers. If the tension and friction are sufficient the web will move with a tangential velocity that is equal to that of the roller surfaces.

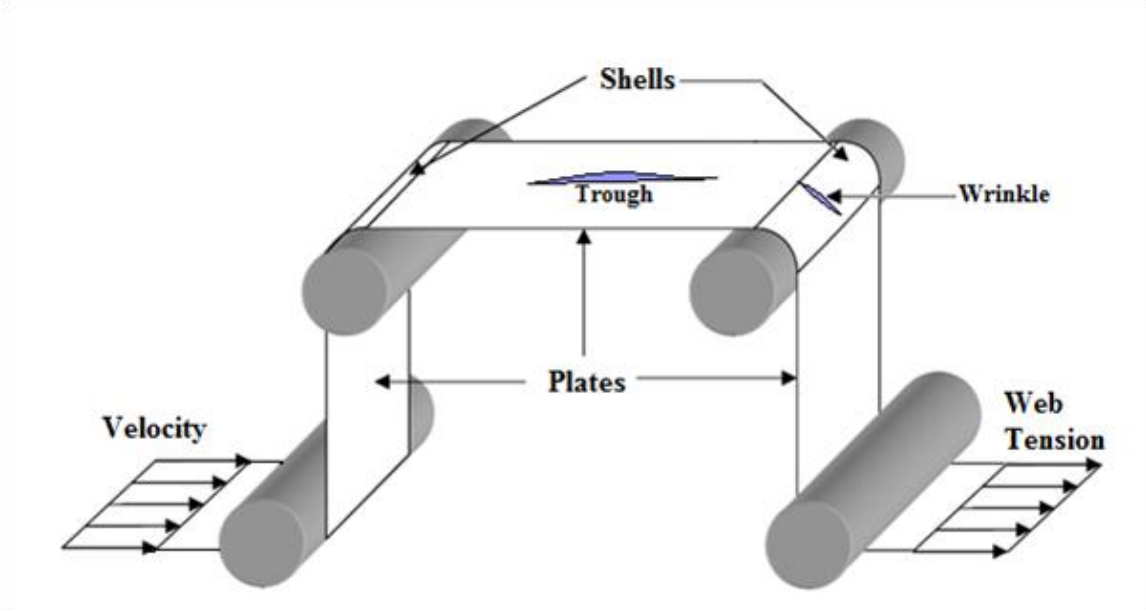

Figure 1 - Web in Transport through Process Machine

The boundary conditions for problem of instability of webs might appear to depend on the frame of reference of the observer. If the observer is moving with the web it will appear to be a moving boundary condition problem as the unsupported plates of web becomes cylindrical shells as they transit rollers and then become a plate again. In the second case if the observer is standing to the side of the machine, the plates and shells

appear to have fixed dimensions and have steady state boundary conditions even though the web is moving. Due to the negligible mass of web the dynamic forces associated with the moving boundary conditions are small and can be neglected. Therefore here boundary conditions are defined with reference to second observer. In this problem the plates are supported at two opposing ends by rollers. The other two edges of plates are unsupported. The rollers give contact support to shells but this support is insufficient to prevent buckling instability of the shell.

Webs exhibit multiple behaviors in terms of stability. The ideal behavior would be a stable web. In this case there would be no out-of-plane deformation of the plates, and also the shells would be perfectly cylindrical in shape. The second type of behavior is called troughs. Troughs are out-of-plane deformations of the web span between two rollers. Troughs often occur in web lines with or without wrinkles and may or may not be detrimental to the web quality depending on whether a process requires the web to be flat or not. The third type of behavior is called wrinkles. Wrinkles are out-of-plane deformations of the web that are transferred over rollers from one span to the next. Wrinkling is the most common defect encountered in manufacturing and converting of lightweight webs. The wrinkles are much more detrimental than troughs as they may cause creases, fold-overs and bursts which can degrade or even stop operations like coating, printing and paper-making. The web handling industry is continuously working on minimizing reasons responsible for wrinkling in order to improve the product quality with minimum waste.

The direction of the web travel through process machinery is called the Machine Direction (MD) and the coordinate direction normal to the machine direction in the plane of the web is called the Cross-Machine Direction (CMD). CMD lateral forces are mainly responsible for troughs and wrinkle formation. If the compressive CMD forces increase, an in-plane compressive second principal stress is produced and also increases (i.e. it becomes more negative). When this second principal stress reaches a critical value for buckling given by Shelton [1] troughs will start to appear in the web. The critical CMD compressive stress required to buckle the isotropic web under MD tension in free span can be calculated using the following equation:

$$\sigma_{cr} = \frac{-\pi h}{a}\sqrt{\frac{\sigma_{md} * E}{3(1-\nu^2)}} \qquad \{1\}$$

where h is the thickness of the web, a is the length of web span, σ_{md} is the tensile stress in web due to web line tension, *E* is the isotropic elastic modulus of the web material and ν is Poisson's Ratio.

Similarly the critical CMD stress required to induce wrinkles in cylindrical shells is given by Timoshenko [21] as:

$$\sigma_{cr} = \frac{-hE}{R\sqrt{3(1-\nu^2)}} \qquad \{2\}$$

where R is the Radius of the Roller.

Wrinkles resulting from lateral shear forces are termed as Shear Wrinkles. The main causes of shear wrinkles in process industry include misaligned rollers, tapered rollers and other roller or web imperfections.

1.2 Web Non-uniformity

Depending on the final product requirement sometimes webs may have non-uniformities like thickness variation across the web width or voids. Some products require layers of different materials to be bonded together (i.e. laminated) to meet the desired characteristics of the final product. Also there are many limitations associated with the production of webs that prevents the web from being perfectly uniform in length and thickness. This research study focuses on how non-uniform webs differ from uniform webs in terms of instability. Much of the research to date has focused on instabilities in uniform webs. Little is known regarding whether non-uniform webs are more or less stable than uniform webs which will be examined herein.

CHAPTER II

Review of Literature

2.1 Journal Papers and Articles

Shelton [1] was one of the first to study the theory governing the lateral dynamics of webs travelling through process machines. He studied the steering of a web due to a misaligned downstream roller. He developed some fundamentals of web behavior such as the zero internal web moment in a web approaching a downstream roller in a web span and the development of a slack edge criterion. Shelton also stated the principle of normal entry of a web approaching a downstream roller. These concepts were very important in establishing the correct boundary conditions for a web moving toward a downstream misaligned roller. Shelton modeled the web between two rollers as a beam. Then he applied the boundary conditions in order to satisfy the principles stated above to calculate the lateral web deflection. Shelton also built a test setup for experimental verification of his proposed model.

Miller and Hedgepeth [2] developed a wrinkling algorithm for finite elements based on the Stein-Hedgepeth wrinkle model. A local elasticity matrix D is developed for each finite elements based on their current strain state in each element. Each element may exhibit taut, wrinkled or slack behavior depending on the current state of strain. The finite element stiffness matrices were used in non-linear analyses of membrane structures. The external loads were applied in small increasing increments. After the element strains were calculated for a previous load increment the effective local elasticity matrices were updated based on the state of strain in each element using the algorithms presented in expressions {3}. After few load increments the local elasticity matrices were revised iteratively until resulting local stresses and strains in every element were in equilibrium. This procedure was continued until the final external loads were achieved and convergence was obtained.

$$
\begin{aligned}
\boldsymbol{D_{slack}} &= \begin{bmatrix} \mathbf{0} & \mathbf{0} & \mathbf{0} \\ \mathbf{0} & \mathbf{0} & \mathbf{0} \\ \mathbf{0} & \mathbf{0} & \mathbf{0} \end{bmatrix} && ; && \boldsymbol{\varepsilon_2 \le \varepsilon_1 \le 0} \\
\boldsymbol{D_{wrinkle}} &= \frac{\boldsymbol{E}}{\boldsymbol{1-\lambda^2}} \begin{bmatrix} \mathbf{1} & \boldsymbol{\lambda} & \mathbf{0} \\ \boldsymbol{\lambda} & \mathbf{1} & \mathbf{0} \\ \mathbf{0} & \mathbf{0} & \frac{\boldsymbol{1-\lambda}}{\mathbf{2}} \end{bmatrix} && \boldsymbol{where\ \lambda = \frac{-\epsilon_2}{\varepsilon_1}}; && \boldsymbol{0 < \varepsilon_1\ and\ \nu\varepsilon_1 < -\varepsilon_2} \qquad \{3\} \\
\boldsymbol{D_{Taut}} &= \frac{\boldsymbol{E}}{\boldsymbol{1-\nu^2}} \begin{bmatrix} \mathbf{1} & \boldsymbol{\nu} & \mathbf{0} \\ \boldsymbol{\nu} & \mathbf{1} & \mathbf{0} \\ \mathbf{0} & \mathbf{0} & \frac{\boldsymbol{1-\nu}}{\mathbf{2}} \end{bmatrix} && ; && \boldsymbol{0 < \varepsilon_1\ and\ \nu\varepsilon_1 > -\varepsilon_2}
\end{aligned}
$$

This algorithm was easy to adapt in any finite element code with iterative non-linear capability.

Friedrich and Good [3] investigated the structural behavior of a web wrinkle passing over a cylindrical roller using finite element technique. They determined the relative effects of several material and geometric parameters on wrinkle stability based on assumption of material homogeneity and isotropy. The effect on wrinkling stability was studied by varying each processing parameter separately while holding other parameters constant. This study was useful for setting corrective guidelines to avoid problems like web tearing and longitudinal creasing.

Gehlbach et al. [4] established a failure criteria equation for predicting the onset of shear troughs in a free span of a web, under the condition that the web was not allowed to slip at the roller immediately upstream of the misaligned roller. This paper was focused on Timoshenko's Plate Buckling criteria [21], which suggested that shear stresses coupled with web line tension could result in a compressive 2^{nd} principal stress responsible for buckling of web. The mathematical model presented here was supported by experimental verification for the case of the misaligned downstream roller. The experiments were performed for different aspect ratios (a/b), web caliper (thickness) and web line velocity.

Gopal and Kedl [5] developed finite element models to predict the formation of troughs and shear wrinkles. Their model extends the plate buckling theory to include slack edge behavior in the web and does not limit the trough shape to uniform amplitude sine waves. They too assumed that no moment was transferred into up-stream spans.

They performed finite element analysis using two approaches; in the first approach the web was modeled by two dimensional wrinkling membrane elements in which the elements do not have any capacity to resist compressive stresses. In this analysis total shear force is applied in one load step and equations iterated to achieve an equilibrium condition to determine the lateral deformation at downstream roller. In order to determine the condition for wrinkling, the shear force was increased until an unstable equilibrium equation was produced. But this model was unsuccessful in predicting wrinkles.

The second approach that was used to model the web used three dimensional plate elements that allowed out-of-plane deformation of the web. The misaligned roller was simulated by adding shear force in the CMD, after that a small out-of-plane perturbation was introduced into the model to establish an out-of-plane web shape. The troughs were said to be formed if there was out-of-plane deformation remaining after the out-of-plane perturbation force was removed. This model was able to successfully predict both lateral deformation of web and wrinkle failure. The model was tested against experimental results for producing the web shape for various misalignments and for wrinkles. They did not compared results with any classical shell-buckling theory. The web in shell form while on the roller was not modeled in any way which prevented wrinkle analysis.

Papandreadis [6] presented a finite element code using wrinkling membrane elements which cannot support either bending or compression. He applied the lateral forces to model and characterized the effects of various material properties, loading

conditions and web thickness on web wrinkling. He also studied the lateral contraction of the web width. The algorithm was developed for calculation of average trough amplitude. Also presented in the paper was a buckling analysis of panels in NASTRAN and the characterization of the resulting mode shapes, including the number of waves present and wavelengths of the corrugations. The boundary conditions incorporated into the model were unable to simulate the process of web travelling over the roller surface; therefore this model was unable to predict the actual web behavior over a roller.

Shelton [7] studied the buckling of webs in free span and rollers due to lateral compressive forces. He developed the buckling criteria for web on roller as a pressurized cylindrical shell and web under tension in free span. He used Timoshenko's buckling theory [21] to derive relationship between apparent buckling strain as a function of the ratio of amplitude and wavelength of buckled web. Shelton also analyzed the wrinkling behavior of a web due to change in tension across a roller, temperature or moisture level. He also considered the visco-elastic memory of plastic web, bending of wound rolls and roller deflections as possible sources of compressive strains.

Bensen et al. [8] developed a finite element code to simulate wrinkling patterns in a web due to non-uniform transport conditions. They examined wrinkling of very thin webs under different edge displacement conditions. The code was based on the tension field theory. They developed a Finite Element code with Wrinkling Analysis (FEWA) by utilizing the wrinkling strain method which assumed that out-of-plane deflection relieves

compressive stress across a wrinkle and that there is strain associated with this deflection. The algorithm was modified depending upon whether individual element exhibit taut or wrinkled behavior. The code was employed to give useful design information regarding the locations of compressive stresses and location of wrinkles if compression is relieved through buckling. The program was unable to predict onset of troughs or wrinkling wavelengths.

Good [9] predicted the shear in multi-span web system. He showed the effect of traction variation on the moment transfer between multiple web spans. The structural stiffness matrix approach given by Przemienecki [20] was used to calculate the moment due to a downstream misaligned roller and it was then compared with the moment which could be supported by friction between the web and roller. He also included the variation in traction due to entrained air between a moving web and transport roller. Good also developed slack edge criteria for a misaligned roller. The expressions developed in the paper for web shear and deformation as a function of roller misalignment, moment transfer and web edge slackness were verified experimentally for different materials.

Good et al. [10] discussed another work related to shear wrinkling in isolated web spans by applying classical instability theory. He modeled the problem to show dependence of wrinkles on the available traction between web and roller surface. Both Regime 1 (velocity independent) and Regime 2 (velocity dependent) wrinkles were modeled analytically and verified experimentally wherein traction was expressed as a

function of entrained air. The model was successful in determining the out-of-plane buckled deformations in free span i.e. troughs. In the case of Regime 2 wrinkles a traction algorithm, dependent on roller and web surface roughness, roller radius, static coefficient of friction, web tension and velocity, was developed as a function of air film thickness. The proposed model was able to predict Regime 1 shear wrinkles and compute a minimum level of machine direction tension required to propagate any wrinkle across the roller.

Good and Straughan [11] proposed a closed form solution for predicting wrinkles due to web twist. To determine the analytical solution the Rayleigh-Ritz method was employed to develop the stress profiles throughout the membrane using an Airy stress function. The CMD stress from analysis was equated to critical value required to buckle the cylindrical shell of web upon the roller surface to predict the onset of wrinkles. The theory presented was verified experimentally for range of materials.

Webb [12] used finite element methods to predict the web wrinkles due to misalignment of a downstream roller in a web span. This model was also verified experimentally. He used the wrinkling membrane elements to model the free span.

Hashimoto [13] developed a theoretical model for predicting generation of web wrinkling due to misalignment of the roller and friction characteristics between web and

roller based on the observation for anisotropic webs. The model was verified by comparing results with measured data for various operating parameters.

Brown [14] proposed models for lateral mechanics of webs encountering misaligned and tapered roller. The model was based on two modified boundary conditions. One was a generalization of normal entry rule. The other was based on the application of principle of conservation of mass and was called the normal strain rule. Using these two rules along with a non-linear version of the equations for two-dimensional plane stress numerical solution was obtained with a finite element partial differential equation solver. The results were compared with previously developed models.

Beisel [15] developed finite element models in COSMOS to predict troughs and wrinkles in uniform webs approaching tapered and misaligned rollers. He also derived analytical expressions for critical taper and critical misalignment required for trough formation. In his finite element models he implemented the boundary conditions established by Shelton [1], including the normal entry rule. The taper of roller or misalignment was simulated by applying shear forces in the CMD. He used the COSMOS® adaptation of the wrinkling membrane elements developed by Miller and Hedgepeth [2] to model the free span of web between two rollers. The non-linear analysis of the model was performed to predict the onset of wrinkles by gradually incrementing the shear force. The analysis was repeated until critical buckling stress was reached. He

verified and applied the shell buckling criteria to model the web on roller. Both tapered and misaligned roller models were verified by detailed experimentation and the comparison of results was satisfactory. Beisel's study was first in the literature in presenting a method by which both troughs and wrinkles in webs could be predicted.

Beisel et al. [18] employed classical instability analysis to predict onset of buckling called troughs in the web. The non-linear finite element analysis was used to model the tension field behavior of the web and to predict when the stiffeners that divide the webs will buckle or wrinkle. They verified model by conducting experiments with misaligned and tapered rollers. They also proposed a model to predict onset of troughs and wrinkles due to crowned downstream roller and achieved good agreements with experimental results.

Mallya [16] investigated effects of voids like circular or elliptical hole on stability of webs. Voids in webs may occur as a result of the formation process or sometimes they are intentionally cut to satisfy the needs of a final web product. As voids in a web approach a downstream roller troughs form which may induce wrinkles. The CMD compressive stresses in the web on the roller become more compressive as the void and the associated troughs near the roller. Mallya demonstrated how these cases could be modeled using the finite element techniques outlined by Beisel [15]. He also verified the results experimentally.

Kara [17] developed finite element model to predict wrinkles in webs with non-uniform length across the width. The finite element modeling method used by Beisel [15] to model wrinkling due to misaligned, tapered and crowned rollers was modified to predict the occurrence of wrinkles due to length non-uniformity. The model was verified experimentally. The length variation across the web width was simulated using the thermo-elastic response of the web to a temperature distribution.

2.2 Research Objective

Beisel demonstrated a method which was proven to successfully model troughs and wrinkles in uniform webs due to misaligned, tapered and crowned rollers. Mallya was successful in demonstrating that the same method could be applied to web wrinkles due to voids. Kara was successful in demonstrating the same method could be successfully applied to web wrinkles due to web length variation.

The objective of this research will be to determine if the methods developed by Beisel for predicting troughs and wrinkles in uniform webs can be applied to webs with non-uniform web thickness across the web width. If successful these methods will be used to compare the propensity for non-uniform webs to trough and wrinkle in comparison to uniform webs.

CHAPTER III

Analytical Model Development

3.1 Preliminary Assumption

Herein the propensity for non-uniform webs to trough or wrinkle will be considered. In this analysis the non-uniformity will be restricted to a web that has a step in uniform thickness part way across the web. This type of non-uniformity is common for laminated webs. This being said there are certainly choices in how webs are laminated. It will be assumed that the two laminae have been strain matched prior to lamination. This ensures that the laminated material will lie flat in the unloaded state. It also ensures that no internal web moments will pre-exist in the web.

3.2 Non-uniform Webs

In this study the non-uniformity of a web cross-section is considered. An analytical model is presented here to study the formation of troughs in a web with a step change in thickness. A step web induces a lateral shear force into the web. Due to this force the web will be steered laterally and there will be formation of CMD compressive stress which can lead to the formation of troughs and wrinkles in the web. In this case the stiffness matrix approach, previously used by Beisel [15], is used by considering an isolated web span as a beam to determine the deflection of the beam. The two cases of a step web approaching a tapered roller and a misaligned roller are taken into consideration here. The compressive stresses due to the step thickness change will combine with compressive stresses due to downstream roller taper or misalignment. Thus the troughs and wrinkles may now be the combined result of web and roller imperfections.

Beisel [15] analyzed a uniform web encountering a tapered and a misaligned roller. He developed closed form solutions for the critical taper and the critical misalignment required for trough formation in uniform webs:

$$m_{cr} = \frac{2aR\left[60E_xI+Ta^2(1+\phi)\right](T+GA_S)}{3b^2E_xGA_S[10E_xI+Ta^2(1+\phi)]}\sigma_{ex} \qquad \{4\}$$

$$\theta_{cr,\tau_{avg}} = \frac{6(5b^6{E_x}^2h^2 + a^4T(5bGh+3T)(1+\phi) + a^2b^3E_xh\left(25bGh+T(6\phi-4)\right))}{5G(5b^6{E_x}^2h^2 + 9a^4T^2(1+\phi) + 2a^2b^3E_xhT(13+3\phi))}\sigma_{ex} \qquad \{5\}$$

where $$\sigma_{ex} = \sqrt{\sigma_{ycr}\,(\sigma_{ycr} - \frac{T}{bh})}$$

Beisel [15] demonstrated the efficacy of the expressions by using a test setup with an isotropic polyester web. The derivation for the uniform web given by Beisel [15] was verified and is used for comparison with the non-uniform web theory presented herein. Beisel's expressions {4} and {5} account for tension stiffening which is important for long spans and shear stiffening which is important for short spans.

3.3 Web Deflection Due to Tapered Roller

It is not always possible to manufacture perfectly cylindrical rollers. Manufacturing error produces rollers with an unintentional radial taper. These tapers will have detrimental effect on the webs encountering the roller, producing troughs and wrinkles due to shear. Modern manufacturing techniques may be helpful in minimizing the errors, but are costly. Therefore it is necessary to study the effect of a taper on the web line and providing guidelines and setting tolerance limits for roller manufacturing.

It is assumed that when a non-uniform web passes over a tapered roller that the bottom of web and the roller surface will share a common velocity that can vary with CMD location. A high web to roller coefficient of friction is assumed and as a result the web span under study will be isolated from moments in other spans. Insufficient web to

roller traction will result in the bending moment transfer from one span to another across a roller.

To study the effects of web non-uniformity a web with simple thickness non-uniformity has been chosen. The web will have the regions of constant web thickness that transition as a step part way across the web width. This was done to simulate a laminated web.

3.4 Properties of Non-uniform Webs

h_1 = thickness on the thinner side of the web

h_2 = thickness on the thicker side of the web

b = total width of the web

b_1 = width of thicker section of the web

$h_o = h_2 - h_1$

b_c = distance of the centroidal axis from the thinner side= $\frac{\frac{h_1(b-b_1)^2}{2}+b_1h_2[b-\frac{b_1}{2}]}{A}$

A = area of the cross section= $[(h_1 * b) + (h_o * b_1)]$

Q = first moment of area at given location

I = moment of inertia of a step cross-section

$$I = \frac{h_1 * b^3}{12} + \frac{h_o * {b_1}^3}{12} + (h_1 * b) * (\frac{b}{2})^2 + (h_o * b_1)\left[b - \frac{b_1}{2}\right]^2 - [(h_1 * b) + (h_o * b_1)]{b_c}^2 \quad \{6\}$$

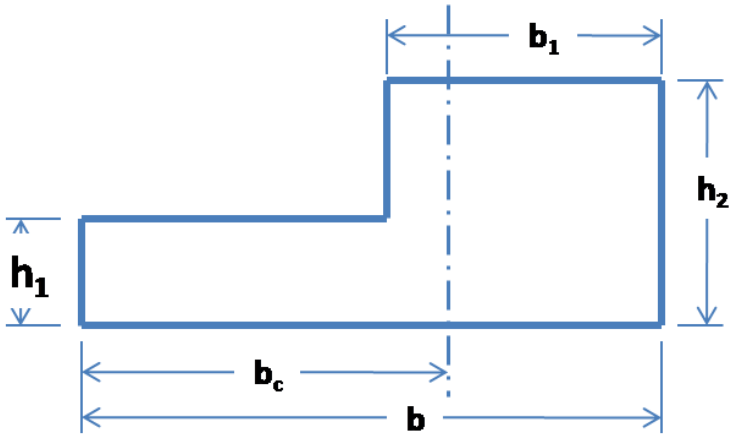

Figure 2 - Cross-section of Step Web

3.5 Boundary Conditions

A step web moving on a tapered roller has a surface velocity profile on its lower surface that varies proportionately with the radius of roller. Due to the frictional forces between the web and the roller surface the lower surface of the web will confirm to the velocity profile of the roller. Since the web has a step thickness change in its cross-section one side of the web will move faster over further distance than other side of the web. This difference of velocity will generate the moment across the width of the web. In this case some additional moment will be generated by the web.

The radius of the roller is given by expression {7}, where 'R' is the nominal radius at the center, 'm' is the slope of the radial taper (in/in) and 'y' is the CMD position across the roller with its origin at the center.

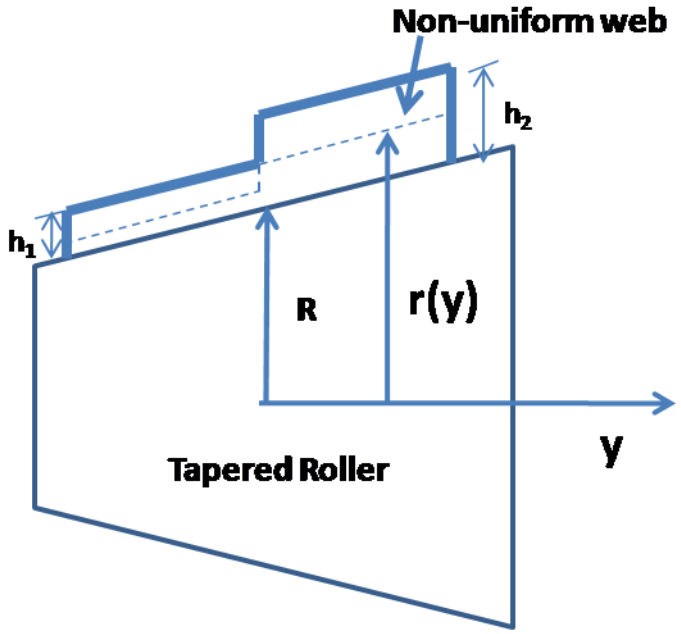

Figure 3 - Tapered Roller Profile with Non-uniform Web

$$r(y) = m * y + R$$

For the thin edge: $r_1(y) = m * y + R + \frac{h_1}{2}; \quad -b_c < y < -b_c + (b - b1)$

For the thin edge: $r_2(y) = m * y + R + \frac{h_2}{2}; \quad -b_c + (b - b1) < y < b - b_c$

{7}

The local and average velocities of the web are given by expression {8} in which '*V*' is the tangential velocity of the web and 'ω' represents the angular velocity of the roller.

$$V_1(y) = r_1(y) * \omega = [m * y + R + \frac{h_1}{2}] * \omega$$
$$V_2(y) = r_2(y) * \omega = [m * y + R + \frac{h_2}{2}] * \omega \quad \{8\}$$
$$V_{avg} = R * \omega$$

In this case if we consider two sections with different thicknesses separately, we can write expressions for the strain profile of the respective section due to the difference in velocity across the width of the web. This analysis does not take into account any additional strain and stress due to the web line tension.

$$\varepsilon_{md}\ (y) = \frac{V(y) - V_{avg}}{V_{avg}}$$
$$\sigma_1(y) = E_x * \varepsilon_{md\,1}\ (y) = \frac{E_x * [m * y + \frac{h_1}{2}]}{R} \quad \{9\}$$
$$\sigma_2(y) = E_x * \varepsilon_{md\,2}\ (y) = \frac{E_x * [m * y + \frac{h_2}{2}]}{R}$$

The moment induced by a step web is calculated by integrating the varying stress across the width of the web.

$$M_j = \int_{-b_c}^{-b_c+(b-b1)} \left[-\frac{E_x * [m * y + \frac{h_1}{2}]}{R} h_1 y \right] dy + \int_{-b_c+(b-b1)}^{(b-b_c)} \left[-\frac{E_x * [m * y + \frac{h_2}{2}]}{R} h_2 y \right] dy \quad \{10\}$$

where b = web width, h_1 and h_2 = web thickness at the opposite ends of the web, E = Young's modulus, R = roller radius, M_j = moment applied at a downstream roller.

The slope of the beam at the ends gives other boundary conditions like the upstream deflection and the end rotations. The upstream deflection (v_i) can be arbitrarily set to zero. For the Timoshenko beam the rotations of the cross-section at the beam ends is given by expression {11}.

$$\theta_{i,j} = \frac{dv}{dx} + \gamma_{xy} = \frac{f_{yj}}{G*A_s} \quad \{11\}$$

According to the condition of normal entry of a web approaching or exiting a roller requires the slope of the lateral deformation $\frac{dv}{dx}_{i,j}$ to be zero in expression {11}. The rotation at a downstream roller(θ_j) will be zero in order to follow the normal entry of a web on to the roller. Thus $\frac{dv}{dx}$ and$\gamma_{xy}[\frac{\partial u}{\partial y} + \frac{\partial v}{\partial x}]$ must combine in such a way that θ_j becomes zero. The shear strain effect is not considered in Euler beam theory. Thus rotations of the cross-section ($\theta_{i,j}$)and the slope of the beam become synonymous in Euler Theory. Euler theory is used for long span beams (a/b>10) where bending stresses and strains are predominate. Timoshenko beam theory can be applied for beams with or without considering shear effects and is applicable for all span ratios (a/b). This analysis will be done using Timoshenko beam theory.

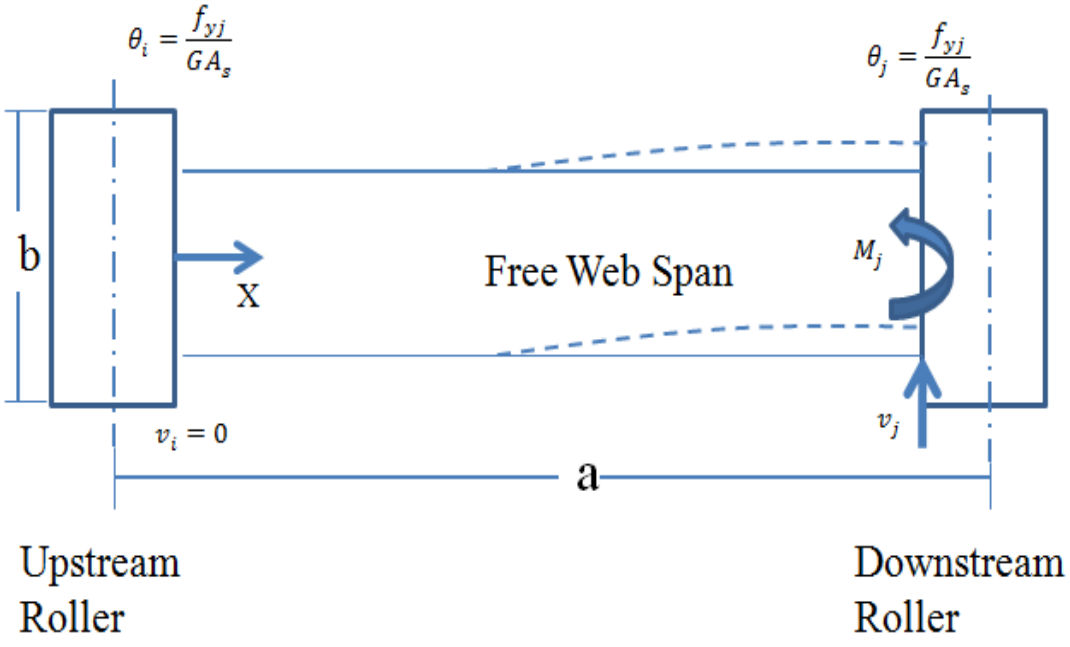

Figure 4 - Boundary Conditions for a Tapered Roller

3.6 Beam Model

The stiffness matrix approach is used to model an isolated web span as a beam. This methodology is demonstrated by Przemieniecki [20]. The stiffness matrix gives the relation between the forces and the elemental deformations. First, the basic stiffness matrix for a simple beam is formed and then terms related to the shear effects are added to the matrix. Finally the matrix is superimposed with another matrix representing the stiffness of a web due to the web line tension. The resulting stiffness matrix is given by expression {12}.

$$\begin{bmatrix} f_{yi} \\ M_i \\ f_{yj} \\ M_j \end{bmatrix} = \begin{bmatrix} \frac{12E_xI}{a^3(1+\phi)} + \frac{6T}{5a} & \frac{6E_xI}{a^2(1+\phi)} + \frac{T}{10} & \frac{-12E_xI}{a^3(1+\phi)} - \frac{6T}{5a} & \frac{6E_xI}{a^2(1+\phi)} + \frac{T}{10} \\ \frac{6E_xI}{a^2(1+\phi)} + \frac{T}{10} & \frac{E_xI(4+\phi)}{a(1+\phi)} + \frac{2Ta}{15} & \frac{-6E_xI}{a^2(1+\phi)} - \frac{T}{10} & \frac{E_xI(2-\phi)}{a(1+\phi)} - \frac{Ta}{30} \\ \frac{-12E_xI}{a^3(1+\phi)} + \frac{6T}{5a} & \frac{-6E_xI}{a^2(1+\phi)} - \frac{T}{10} & \frac{12E_xI}{a^3(1+\phi)} + \frac{6T}{5a} & \frac{-6E_xI}{a^2(1+\phi)} - \frac{T}{10} \\ \frac{6E_xI}{a^2(1+\phi)} + \frac{T}{10} & \frac{E_xI(2-\phi)}{a(1+\phi)} - \frac{Ta}{30} & \frac{-6E_xI}{a^2(1+\phi)} - \frac{T}{10} & \frac{E_xI(4+\phi)}{a(1+\phi)} + \frac{2Ta}{15} \end{bmatrix} \begin{bmatrix} v_i \\ \theta_i \\ v_j \\ \theta_j \end{bmatrix} \quad \{12\}$$

The sign conventions used for the deformations, forces and moments are as represented in figure 5.

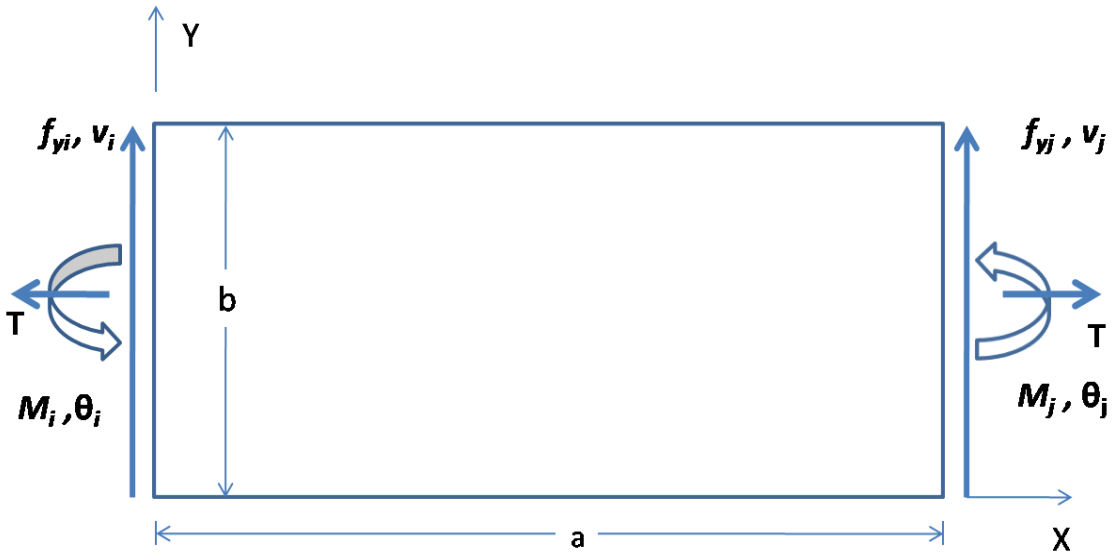

Figure 5 - Positive Sign Conventions of Beam

The shear effect is represented by term 'ϕ' in expression {12} and is defined by expression {13}:

$$\phi = \frac{12E_x I}{GA_s a^2} \qquad \{13\}$$

where E_x is Young's modulus in MD, I is moment of inertia of the cross-section, A_s is area of the cross-section reacting shear = (5/6)*(Area of Web) [Assumed].

After applying the boundary conditions discussed earlier and expanding the 3rd and 4th rows of expression {12}, we can develop a model for describing the behavior of a web encountering a tapered roller. Expanding the 3rd row in expression {12} and solving for f_{yj} gives the following expression:

$$f_{yj} = \frac{6GA_s[10E_x I + Ta^2(1+\phi)]v_j}{a[60E_x I + a^2(T+5GA_s)(1+\phi)]} \qquad \{14\}$$

Similarly, expanding the 4th row of expression {12} will give the moment developed at a downstream roller. If we substitute θ_i and $v_i = 0$, we can solve it for lateral force f_{yj} :

$$f_{yj} = \frac{GA_s\{10a^2(1+\phi)M_j + [60E_xI + Ta^2(1+\phi)]v_j\}}{a[60E_xI + Ta^2(1+\phi)]} \quad \{15\}$$

Expressions {14} and {15} both represent the downstream shear force (f_{yj}), therefore we can set them equal to each other and resulting expression can be solved for the downstream deflection v_j given by expression {16}.

$$v_j = \frac{[120E_xI + 2a^2(T+5GA_s)(1+\phi)]M_j}{[60E_xI + Ta^2(1+\phi)](T-GA_s)} \quad \{16\}$$

Expression {16} provides us with the lateral steering of a web due to a downstream tapered roller. Similarly the shear force at a downstream roller may be found by eliminating v_j and solving for f_{yj}. Once again expanding the 3rd row of the stiffness matrix and solving it for v_j gives:

$$v_j = \frac{af_{yj}[60E_xI + a^2(T+5GA_s)(1+\phi)]}{6GA_s[10E_xI + Ta^2(1+\phi)]} \quad \{17\}$$

Similarly, expanding the 4th row of expression {12} will give the moment developed at a downstream roller. If we substitute θ_i and $v_i = 0$, we can solve it for lateral deflection v_j :

$$v_j = \frac{a}{GAs}\left\{\frac{[-10aGA_s(1+\phi)M_j] + [60E_xI + Ta^2(1+\phi)]f_{yj}}{[60E_xI + Ta^2(1+\phi)]}\right\} \quad \{18\}$$

Now by equating expressions {17} and {18} and solving it for the shear force f_{yj}:

$$f_{yj} = \frac{[12GA_s]*[10E_xI+Ta^2(1+\phi)]M_j}{[T^2a^3(1+\phi)]-GA_sTa^3(1+\phi)+[60E_xIa(T-GA_s)]} \quad \{19\}$$

Expressions {16} and {19} yield the deflection of a web and the shear force developed at a downstream tapered roller, in terms of the properties of a web and actual conditions present in the web line.

3.7 Web Instability

The instability criterion for this type of beam model was developed by Good [19]. This analysis can be extended to the web with orthotropic material properties by using expression {20}. Timoshenko's model of a plate loaded along both axis combined with the orthotropic web properties proposed by Lekhnitskii [24] are used to develop an expression for the critical CMD compressive stress for a web span loaded in tension in MD. But in this study only isotropic web materials are considered. So 'E_y' is replaced by 'E' or 'E_x' and $\nu = \nu_{xy} = \nu_{yx}$ in expression {20} to get the critical CMD compressive stress for isotropic web.

$$\sigma_{cr} = \frac{-\pi h}{a}\sqrt{\frac{\sigma_{md}*E_y}{3(1-\nu_{xy}\nu_{yx})}}; \quad Orthotropic$$
$$\sigma_{cr} = \frac{-\pi h}{a}\sqrt{\frac{\sigma_{md}*E}{3(1-\nu^2)}}; \quad Isotropic \qquad \{20\}$$

The MD tensile stress and a CMD shear stress produced due to the steering load f_{yj} are responsible for a compressive second principal stress represented by expression {21}.

$$\sigma_2 = \frac{\boldsymbol{\sigma_{md}}}{\mathbf{2}} - \sqrt{(\frac{\boldsymbol{\sigma_{md}}}{\mathbf{2}})^{\mathbf{2}} + \boldsymbol{\tau}^{\mathbf{2}}} \qquad \{21\}$$

When the principal stress calculated by expression {21} approaches the critical stress at buckling {20} troughs will occur. If we substitute this limit for the principal stress, the critical value of the shear stress which is required to buckle the web can be calculated using expression {22}.

$$\tau_{cr} = \sqrt{[\frac{\pi h}{a}]^2 \frac{\sigma_{md} * E_y}{3(1-\nu_{xy}\,\nu_{yx})} + \frac{\pi h}{a}\sqrt{\frac{{\sigma_{md}}^3 * E_y}{3(1-\nu_{xy}\,\nu_{yx})}}} \qquad \{22\}$$

The shear force f_{yj} can be used to form the maximum shear stress in the web cross-section, which can be further used in principal stress relation given by expression {21}. The maximum shear stress in a step cross-section can be calculated using the same approach as used in case of a rectangular cross-section. For the rectangular cross-section the shear stress distribution is given as:

$$\tau = \frac{6\mathrm{V}}{b h^3}\left\{\frac{h^2}{4} - y^2\right\} \qquad \{23\}$$

Expression {23} shows that the shear stress distribution across the rectangular cross-section is parabolic, having values zero on both the ends and maximum value at the center. The maximum shear stress can be calculated using expression {23} at the center of web (i.e. at y=0).

$$\tau_{max} = \frac{\mathbf{3}f_{yj}}{\mathbf{2}\boldsymbol{A}} \qquad \{24\}$$

Similarly for a step cross-section the shear stress distribution can be calculated as:

$$\tau = \frac{\mathbf{VQ}}{\boldsymbol{It}} \qquad \{25\}$$

where I is moment of inertia of a step web cross-section, V=f_{yj} is total shear force at given location, t is thickness in the material perpendicular to shear, Q is first moment of area at given location. The first moment of area at point of maximum shear stress denoted by shaded lines in Figure 6 will be:

$$Q = h_1(b - b_1)\left[\frac{b-b_1}{2} + b_1 - (b - b_c)\right] \qquad \{26\}$$

If we input all the parameters in expression {25} we can get an expression for the shear stress distribution. Depending on the dimensions of a cross-section we will get different shear stress factors (k).

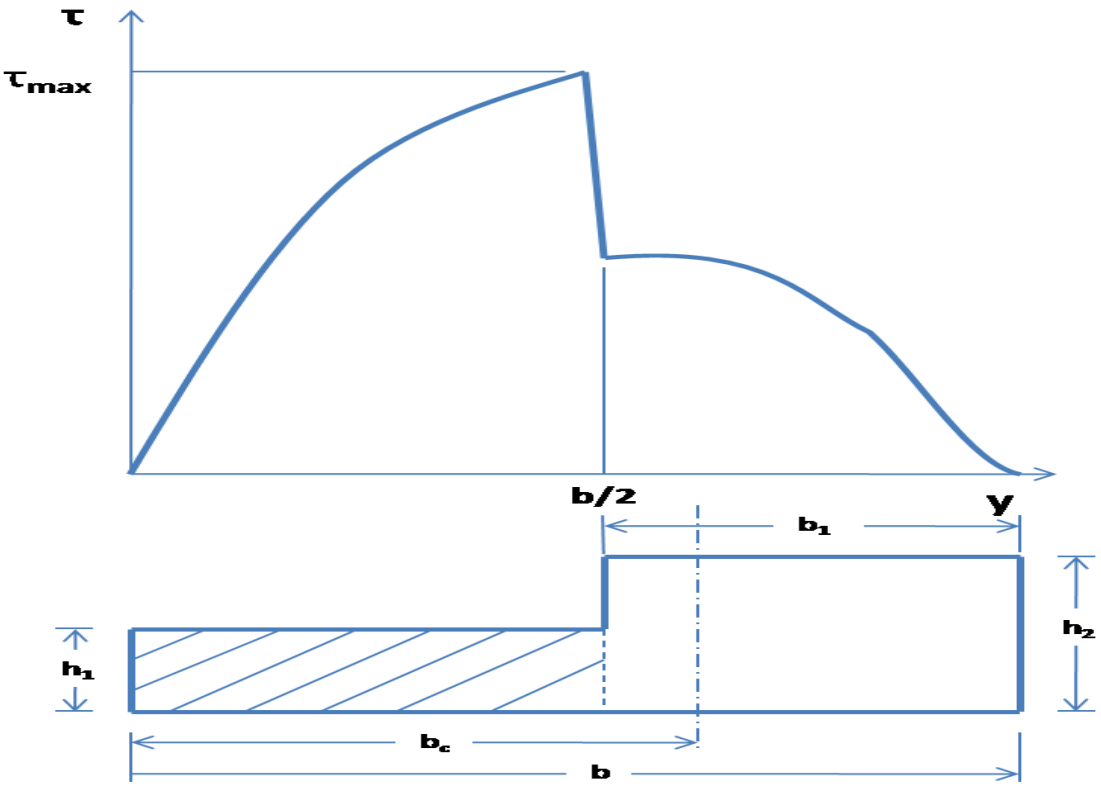

Figure 6 - First Moment of Area corresponding to Maximum Shear Stress

$$\tau_{max} = \boldsymbol{k}\frac{f_{yj}}{\boldsymbol{A}} = \boldsymbol{k} * \tau_{avg} \quad \{27\}$$

k = 1.50 for a rectangular cross-section (Uniform Web)

k = 2.18 for a step cross-section under study (Non-uniform Web)

(b=6, b_1=3, h_1=0.001, h_2=0.002, b_c=3.5)

Use of either average or the maximum shear stress is based on the expected shear stress distribution in the web. If shear force from expression {19} is substituted in expression {27} the result can be solved for a critical radial taper that will induce troughs into a web span. This critical taper is given by expression {28}.

$$m_{cr} = \frac{Rb(h_1+h_2)[60E_xI + Ta^2(1+\phi)]\{[60E_xI + a^2(T-5GA_s)(1+\phi)] - 6[10E_xI + Ta^2(1+\phi)]\}}{12E_xk\left(\int_{-b_c}^{-(b_c-b1)}[h_1y^2]dy + \int_{-(b_c-b1)}^{(b-b_c)}[h_2y^2]dy\right) * 10aGA_s(1+\phi)[10E_xI + Ta^2(1+\phi)]} \sqrt{[\frac{\pi h}{a}]^2 \frac{\sigma_{md} * E_y}{3(1-\nu_{xy}\nu_{yx})}} + \frac{\pi h}{a}\sqrt{\frac{{\sigma_{md}}^3 * E_y}{3(1-\nu_{xy}\nu_{yx})}}$$

{28}

3.8 Web Deflection Due to Misaligned Roller

Roller misalignment in the web handling industry is a critical issue. In the web line all the rollers are aligned in such a way that their axes are parallel. The roller alignment is required to keep the web positioned laterally on a roller and also to avoid trough and wrinkle formation due to the lateral shear force. Accurate roller alignment is very difficult and time consuming process. Proper guidelines and tolerances might be helpful for this process, which can be developed by studying the behavior of a web encountering a misaligned roller.

Good et al [10] and Shelton [1] proposed models for a misaligned roller case. Their models did not include tension effects, shear effects or consideration of orthotropic material properties. Beisel [15] included all these effects while developing his model for the uniform web. The same method is used for a step web encountering a misaligned roller. The behavior of a step web in the web line will depend on properties such as area of cross-section, moment of inertia and first moment of area.

The misaligned roller case is modeled using the structural stiffness matrix approach as used in case of a tapered roller. The web span between an upstream roller and a downstream misaligned roller is modeled as a beam with the sign conventions given by Figure 5. The stiffness matrix for a beam given by expression {12} will be used to describe the web behavior. The properties of a step web cross-section defined in case of a tapered roller will be again used for developing this model. The only difference will be application of the boundary conditions. The boundary conditions in case of a downstream misaligned roller are defined as shown in Figure 7.

The web guide at an upstream roller holds the web entry to arbitrary but constant point which is set to zero.

$$v_i = 0 \qquad \{29\}$$

The rotation at the upstream roller is due to the shear deformation.

$$\theta_i = \frac{f_{yj}}{GA_s} \qquad \{30\}$$

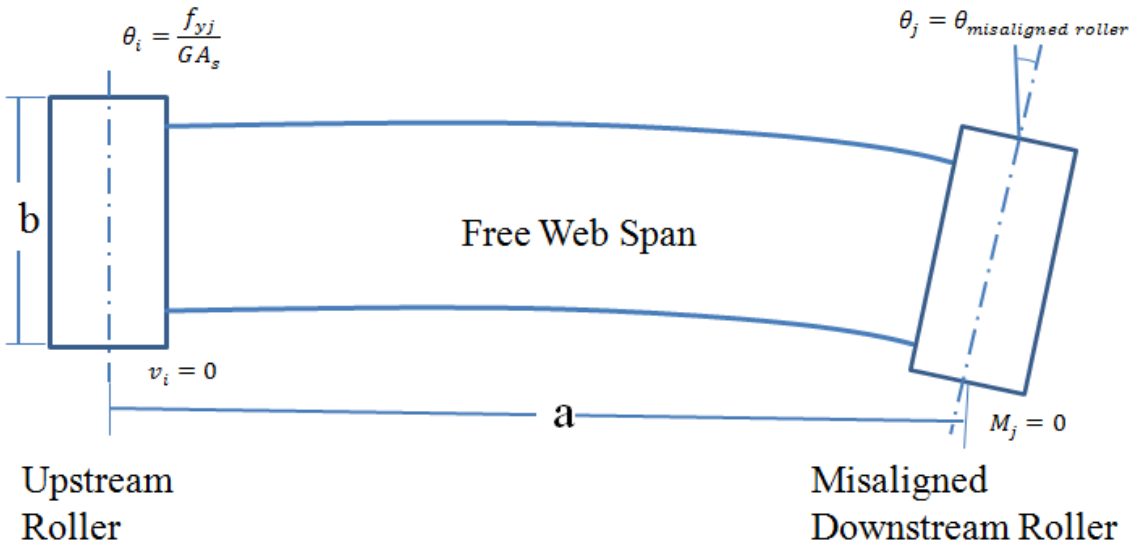

Figure 7 - Boundary Conditions for a Misaligned Roller

The zero moment at a downstream roller was proposed by Shelton [1].

$$M_j = 0 \qquad \{31\}$$

The rotation of the downstream end of a beam will be equal to the angle of roller misalignment.

$$\theta_j = \theta_{misaligned\ \ roller} \qquad \{32\}$$

After applying the boundary conditions discussed earlier and expanding the 3rd and 4th rows of expression {12}, we can develop a model for describing the behavior of a web encountering a misaligned roller. Expanding the 3rd row in expression {12} and solving for f_{yj} gives:

$$f_{yj} = \frac{-GA_s[Ta^3(1+\phi)\theta_j - 12V_j(Ta^2(1+\phi)+10E_xI)]}{a[60E_xI+(Ta^2+10GA_s)(1+\phi)]} \qquad \{33\}$$

Similarly, expanding the 4th row of expression {12} will give the moment developed at a downstream roller. If we substitute M_j, θ_i and v_i from expressions {29-31} we can solve it for lateral force f_{yj}:

$$f_{yj} = \frac{GA_s\{[4Ta^3(1+\phi)+30E_xIa(4+\phi)]\theta_j - V_j[3Ta^2(1+\phi)-180E_xI]\}}{a[Ta^2(1+\phi)-30E_xI(2+\phi)]} \quad \{34\}$$

Expressions {33} and {34} both represent a downstream shear force (f_{yj}), therefore we can set them equal to each other and resulting expression can be solved for the downstream deflection v_j:

$$v_j = \frac{a\{720{E_x}^2I^2+4a^2E_xI[15GA_s(40+\phi)+3T(6+\phi)]+(T^2a^4+8GA_sTa^4)(1+\phi)\}}{3\{240{E_x}^2I^2+8E_xIa^2[15GA_s-T(2-3\phi)]+Ta^4(T+2GA_s)(1+\phi)\}}\theta_j \quad \{35\}$$

Expression {35} provides us the lateral steering of a web due to a downstream misaligned roller. Similarly the shear force at a downstream roller may be found by eliminating v_j and solving for f_{yj}. Once again expanding the 3rd row of the stiffness matrix and solving it for v_j gives:

$$v_j = a\frac{[(Ta^2+10GA_s)(1+\phi)+60E_xI]f_{yj}+[GA_sTa^2(1+\phi)+60E_xI]\theta_j}{12GA_s[10E_xI+Ta^2(1+\phi)]} \quad \{36\}$$

Similarly, expanding the 4th row of expression {12} will give the moment developed at a downstream roller. If we substitute M_j, θ_i and v_i from expressions {29-31} we can solve it for lateral deflection v_j:

$$v_j = \frac{a}{3GAs}\frac{[30E_xI(2-\phi)-Ta^2(1+\phi)]f_{yj}+[4GA_sTa^2(1+\phi)+30GA_sE_xI(4+\phi)]\theta_j}{[60E_xI+Ta^2(1+\phi)]} \quad \{37\}$$

Now by equating expressions {36} and {37} and solving it for the shear force f_{yj}:

$$f_{yj} = \frac{GA_s[240{E_x}^2 I^2 + 8E_x I a^2(13+3\phi) + 3T^2 a^4(1+\phi)]}{240{E_x}^2 I^2 + 8E_x I a^2[15GA_s - T(2-3\phi)] + 2Ta^4(T+2GA_s)(1+\phi)}\theta_j \quad \{38\}$$

Expressions {35} and {38} yield the deflection of the web and the shear force developed at a downstream misaligned roller, in terms of properties of the web and actual conditions present in the web line.

Now if we compare these expressions with that derived by Beisel [15] for a misaligned downstream roller case, we can observe that overall expressions are exactly of the same nature with only difference arising due to the step cross-section instead of a rectangular cross-section for the uniform web. The difference in the cross-section changes the parameters including cross-sectional area, moment of inertia and the first moment of area.

To predict the instability of a web approaching the misaligned roller, the expression describing the behavior of a web must be linked with an instability criterion previously given by expression {20}. This critical buckling stress is equated to the 2nd principle stress given by expression {21} and the result was solved for the critical shear stress, expression {22}. This critical shear stress is now equated to the average shear stress developed due to the shear force. If simultaneously the shear force from expression {38} is substituted in this expression we can solve it for the critical rotation of a downstream misaligned roller, necessary to induce troughs in free span.

$$\theta_{cr} = bh\frac{240{E_x}^2I^2 + 8E_xIa^2[15GA_s - T(2-3\phi)] + 2Ta^4(T+2GA_s)(1+\phi)}{GA_s[240{E_x}^2I^2 + 8E_xIa^2(13+3\phi)+3T^2a^4(1+\phi)]}\sqrt{[\frac{\pi h}{a}]^2\frac{\sigma_{md} * E_y}{3(1-\nu_{xy}\nu_{yx})}} + \frac{\pi h}{a}\sqrt{\frac{{\sigma_{md}}^3 * E_y}{3(1-\nu_{xy}\nu_{yx})}}$$

{39}

3.9 Slack Edge Limitation

If a slack edge is developed in the web, it will limit the use of expressions for the deflection of web and the shear force. A Slack edge occurs when a portion of the web develops zero MD stress. When the MD stress due to the moment becomes equal and opposite to the MD stress due to the web line tension, zero MD stress will develop at a web edge at that location in the web line. The onset of a slack edge can be determined by equating MD stress to zero.

First let us consider the case of the uniform web encountering a misaligned roller. As we know the slack edge forms when portion of a web develops zero MD stress,

$$\sigma_x = \frac{-My}{I} + \frac{T}{A} = 0 \qquad \{40\}$$

For the case of a misaligned roller the model can be considered as a cantilever beam of length ‘a’ with load equal to the shear force ‘f_{yj}’ acting at free end. Therefore the deflection at free end can be given as:

$$v = \frac{f_{yj}\,a^3}{3E_xI} \qquad \{41\}$$

The deflection of a web at a downstream roller can be approximately related to the span length and the degree of misalignment as:

$$v \cong \frac{2a\theta}{3} \quad \{42\}$$

By equating expressions {41} and {42} we get:

$$f_{yj} = \frac{2E_x I\theta}{a^2} \quad \{43\}$$

The moment induced due to this shear force at a downstream roller will be given as:

$$M_j = f_{yj}\, a = \frac{2E_x I\theta}{a} \quad \{44\}$$

Therefore by putting this moment in expression {40} we can get the onset of a slack edge due to a misaligned roller as:

$$\theta_{Slack} = \frac{Ta}{E_x b^2 h} \quad \{45\}$$

By following the same procedure the onset of a slack edge for a misaligned roller can be found for the non-uniform web, the expression for the critical misalignment required in that case can be given by:

$$\theta_{Slack} = \frac{Ta}{2AE_x b_c} \quad \{46\}$$

Similarly the slack edge criteria can be developed for a tapered roller also. In case of a tapered roller with the uniform web, the moment induced at a downstream roller [15] is given by:

$$M_j = \frac{-m E_x h b^3}{12R} \quad \{47\}$$

Putting this moment in expression {40} for the web line stress we will get the critical taper required to develop onset of a slack edge.

$$m_{Slack} = \frac{2TR}{E_x b^2 h} \quad \{48\}$$

In case of the non-uniform web encountering a tapered roller the moment induced is given by expression {10}. If we put this moment in expression {40} we can solve it for the critical taper required to develop onset of a slack edge.

$$m_{Slack} = \frac{TI}{b_c * \left\{ \int_{-b_c}^{-b_c+(b-b1)} \left[-\frac{E_x * [y + \frac{h_1}{2}]}{R} h_1 y \right] dy + \int_{-b_c+(b-b1)}^{(b-b_c)} \left[-\frac{E_x * [y + \frac{h_2}{2}]}{R} h_2 y \right] dy \right\}} \quad \{49\}$$

The expressions developed here gives the critical tension level at which the web will become slack. Thus the analysis of slack edge criteria gives the lowest tension level for a particular misalignment or taper below which wrinkle analysis is not possible.

CHAPTER IV

Finite Element Analysis of Troughs and Wrinkles

4.1 Wrinkles Due to Tapered Roller

When troughs from a free span of the web become severe, out-of-plane deformations begin to traverse a downstream roller and the web is considered to be wrinkled. As a web travels over a roller in the process machine, it changes from the plate structure in the free span to a cylindrical shell on the roller. The shell structure has higher buckling stability than the same web in the tensioned plate form. Therefore the criterion stated in expression {1} cannot be used to predict the critical stress for the buckling of these shell structures. Good and Beisel [19] proved the cylindrical shell buckling criterion developed by Timoshenko, expression {2}, could be used to calculate the critical stress required for the onset of wrinkling.

The wrinkling behavior of the web is difficult to model analytically and there is still no closed form solution available for a wrinkling analysis. Hence FE modeling[1] was used to model the wrinkling behavior observed in the laboratory. Webb [12] was the first one to model the web with troughs formed in the span using finite elements. Webb modeled the behavior of the web encountering a misaligned roller. Webb's model for wrinkling analysis was giving correct results only after adding the angle needed to cause trough formation to the angle of rotation needed to cause wrinkles per FE analysis. Beisel [15] then modified Webb's FE model to predict wrinkles in a misaligned roller as well as a tapered roller case in a consistent manner.

The models developed for a misaligned roller and a tapered roller cases were validated by extensive experimentation for various tension levels and span lengths by Beisel. This shows that Beisel was successful in simulating the actual boundary conditions in both the cases. The method for determination of the onset of wrinkle due to a tapered roller is developed here with some modifications to Beisel's approach. The wrinkling membranes developed by Miller and Hedgepeth [2] are used to handle post buckled state of the web in the free span. As explained earlier wrinkling membrane elements cannot sustain compressive stresses, hence they could be used to model a web with already formed troughs. These elements, when used to handle a buckled condition, may take either elastic or wrinkled or slack state depending on the current state of the strain in the element. Thus it requires a non-linear iterative process to handle the strain state dependent properties of the wrinkling membrane elements.

[1]COSMOSM, SRAC, CALIFORNIA

The FE model developed as shown in Figure 8 is divided into twelve panels. Panels 1-6 represent the thinner side of the web (thickness equal to h_1) and similarly panels 7-12 represent the thicker side of the web (thickness equal to h_2). The first panel represents the web on the upstream roller. This web must be able to contract due to the Poisson effect and the applied tension. As the web exits the upstream roller no slippage is allowed until the web leaves the roller; this is simulated by locking the nodes at the exit of the upstream roller in the x-direction along a vertical line. The nodes in the web on the upstream roller are coupled in horizontal direction to enforce a normal entry and exit. Each node on the horizontal line must move with the same y displacement as the rest of the nodes on the same line. The second panel represents the free web span with potential for developed troughs. The wrinkling membrane elements are used to simulate the buckled state of the web in this span. The third panel represents the web near the end of the free web span approaching a downstream tapered roller and nodes on this panel are again locked in horizontal lines to ensure a normal entry of the web to a roller.

The fourth panel represents the web on a downstream tapered roller. The fifth and sixth panels are used only to help achieve the desired boundary conditions in the left hand side of the model. Similarly panels 7-12 represent the thicker side of the web in same order, seventh panel for the web on the upstream roller, eighth panel for the free web span under study and so on. The boundary conditions represented for the case of a downstream tapered roller as given by expressions {10} and {11}, and $v_i = 0$ are then implemented in the FE model. The set of lateral forces is applied as shown in Figure 8 to impose a constant moment in the web between the entry and exit of a tapered roller. The

web line tension is applied at both the ends of a web using pressure lines, so that it simulates the uniform σ_x stress across the web cross-section. The central node of the model is pinned to constrain the rigid body motion of the web. All rotational degrees of freedom and translation in Z-direction are constrained, so that the web remains planar.

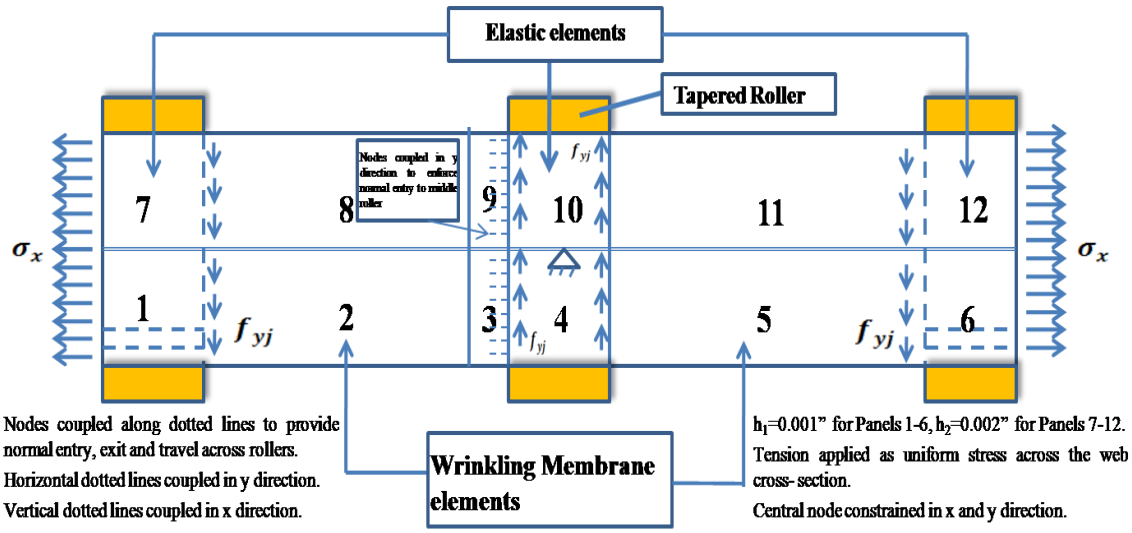

Figure 8 - FE Wrinkle Model, Tapered Roller

Once the model is developed, execution is carried out using the non-linear analysis for prediction of wrinkles and the loads were incremented in 20 time steps. As shown in Figure 9 in the first few load steps the level of the σ_x stress due to web line tension would be raised to desired level. Then shear force would be raised from zero to a test value. After executing the model the compressive principal stresses in elastic elements on the tapered roller were reviewed. While executing the model the shear force was increased in steps until the critical compressive stress given by expression {2} is reached in the second row of elastic nodes on the tapered roller. The second row was

selected due to the way COSMOS interpolates the stresses. COSMOS takes elemental stress values in consideration while interpolating them to nodal stresses. If we select the first row on middle roller, it has an elastic element on one side and a wrinkling membrane element on the other side. The second row of nodes has same type of elements i.e. elastic elements on either side. So interpolation of the nodal stresses gave approximately correct results for the second row of nodes. Once the critical buckling stress {2} is reached the web was considered to have reached the onset of wrinkle formation.

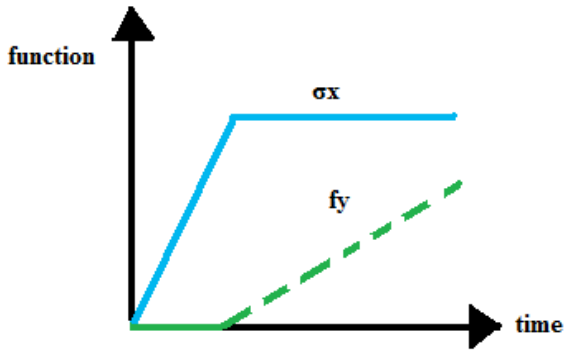

Figure 9 - Time Curve, Non-linear Analysis

When the critical stress is reached the execution of model was stopped and σ_x stresses were recorded for all the nodes on the second row of a tapered roller. This σ_x stresses from the software were compared with theoretical σ_x stresses obtained using expression {40}. The error between these values was minimized by changing the moment using an equation solver. The optimum value of the moment was calculated from this analysis. Finally the critical taper required for the onset of a wrinkle formation was determined by inputting this moment in expression {10}.

Figure 10 shows contours of σ_x from the FE model. By reviewing σ_x stress output we can see that a moment is developed at the upstream end of the troughed web span. The moment decreases linearly until a net value of zero in the middle of the span and continues decreasing towards the downstream tapered roller.

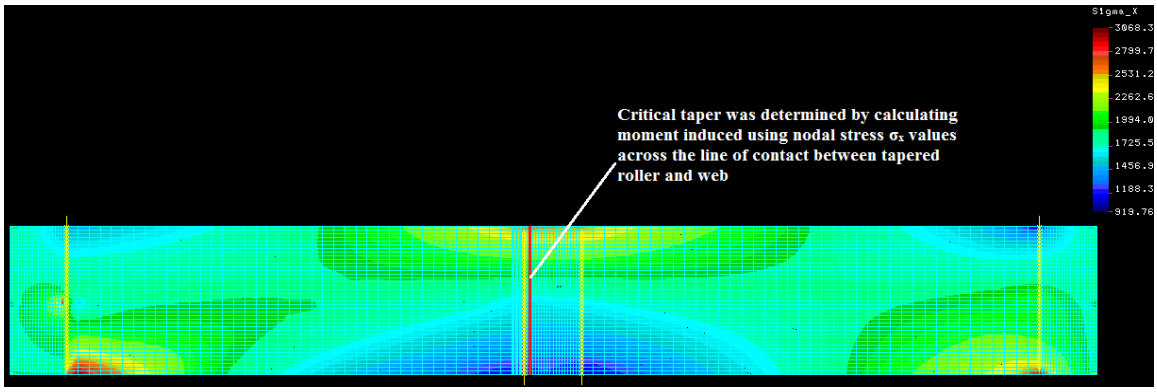

Figure 10 - σ_x Stress Output

The output of the compressive principal stress across the web is shown in Figure 11.

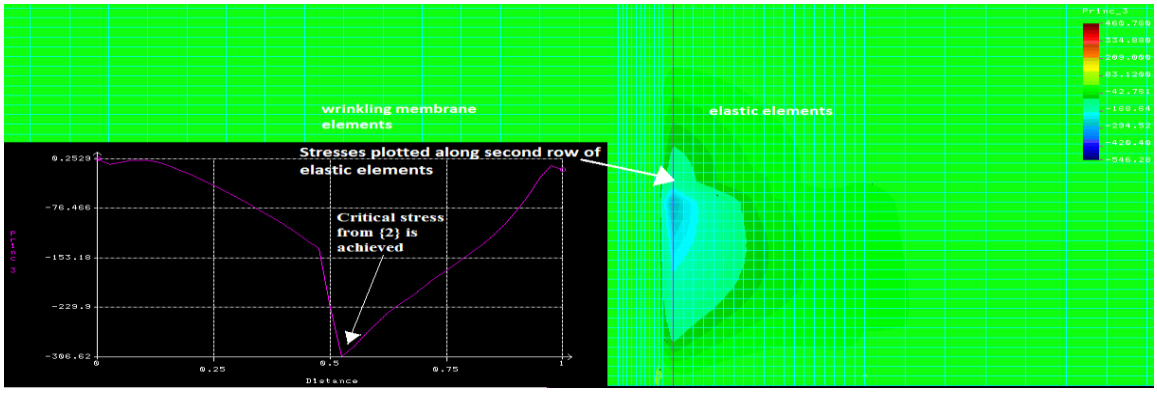

Figure 11 - Critical σ_y Stress developed in FE analysis of Tapered Roller

4.2 Troughs Due to Tapered Roller

The linear analysis of the model described for wrinkles gives the critical taper required for the onset of troughs. The linear analysis was carried out by varying different parameters like the web line tension and aspect ratio. This type of analysis does not take into account the time curves. The σ_x stresses and shear forces both applied directly in a single step. After execution of model σ_2 stresses were reviewed in the middle of a free web span. When these stresses reach the critical value given by expression {1}, troughs are said to be formed. Once this critical principal stress was attained the taper required for the onset of troughs can be calculated using same approach as explained earlier. The results from a linear analysis were compared with the analytical model developed.

4.3 Wrinkles Due to Misaligned Roller

The FE model for determination of the wrinkle formation due to a downstream misaligned roller is similar to the model presented in the previous section. The buckling criterion for a shell given by expression {2}, yields the compressive stress that the web on the misaligned roller can withstand before a wrinkle forms. The boundary conditions presented by expressions {29-32} were implemented in FE model as shown in Figure 12. The moment at a downstream misaligned roller is zero in this case. So the shear forces applied on the middle roller in the case of tapered roller were removed. The model is divided into ten panels. Panels 1-5 represent the thinner side of the web (thickness equal

to h_1) and similarly panels 6-10 represent the thicker side of the web (thickness equal to h_2). The first panel represents the web on the upstream roller. The nodes in the web on the upstream roller are coupled in horizontal direction to enforce a normal entry and exit. Each node on the horizontal line must move with the same y displacement as the rest of the nodes on the same line. This web must be able to contract due to the Poisson effect and the applied tension. As the web exits the upstream roller no slippage is allowed until the web leaves the roller; this is simulated by locking the nodes at the exit of upstream roller in the x-direction along a vertical line. The second panel represents the free web span with potential for developed troughs. The wrinkling membrane elements are used to simulate the buckled state of web in this span. The third panel represents the web on a downstream misaligned roller. The fourth and fifth panels are used only to help achieve the desired boundary conditions in the left hand side of the model.

Similarly panels 6-10 represent the thicker side of the web in same order, sixth panel for the web on the upstream roller, seventh panel for the free web span under study and so on. The web line tension is applied at both ends of the web using pressure lines, so that it simulates the uniform σ_x stress across the web cross-section. The central node of the model is pinned to constrain the rigid body motion of the web. All the nodes are constrained in Z-direction and against rotational degrees of freedom in all three directions, so that the web remains planar.

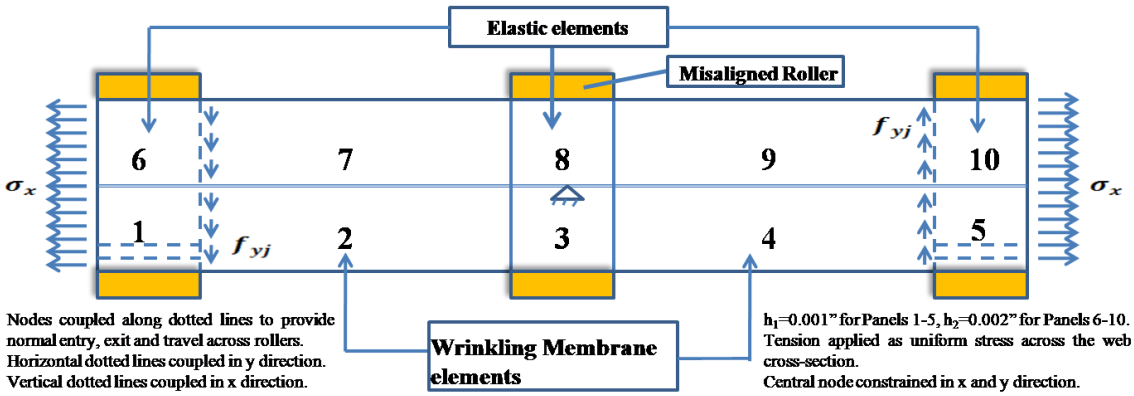

Figure 12 - FE Wrinkle Model, Misaligned Roller

The model was then executed by applying the desired web line tension. In the next step the shear force was applied and increased until the critical compressive stress given by expression {2} was achieved in second row of elements on the downstream misaligned roller (middle roller in model). The shear force and σ_x stresses were applied using time curve as shown in Figure 9. Since the rotational degrees of freedom are not defined for the Shell4 element, the rotation of the downstream roller must be determined through the displacements. Once the critical stress, {2}, was reached, the nodal deformations in Y-direction were recorded for nodes on central horizontal line on middle roller. From these deformations slope was calculated. The misalignment required for the onset of wrinkle formation was then determined as:

$$\theta_j = Arctan \frac{B-A}{Arc\ lengt\ h\ of\ web\ in\ contact\ \ wit\ h\ roller} \qquad \{50\}$$

B = y-deformation on right end of the misaligned roller

A = y-deformation on left end of the misaligned roller

(Points A and B are shown in Figure 13).

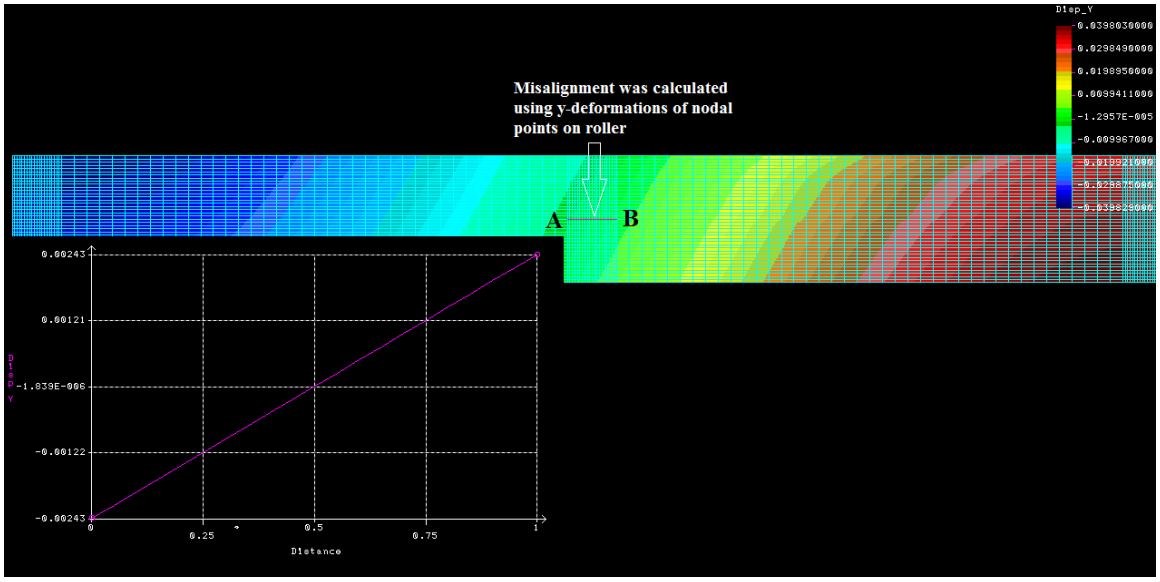

Figure 13 - Deformation across the Misaligned Roller

The sample σ_y stress output from this model is shown in Figure 14. If the MD stress is analyzed we can see a moment varying linearly from maximum at the upstream roller boundary and decreasing as we get towards the downstream misaligned roller. At the downstream misaligned roller the moment reduces to approximately zero. If the deformations across the misaligned roller are studied, it can be seen that web deforms linearly across this region following the normal entry rule.

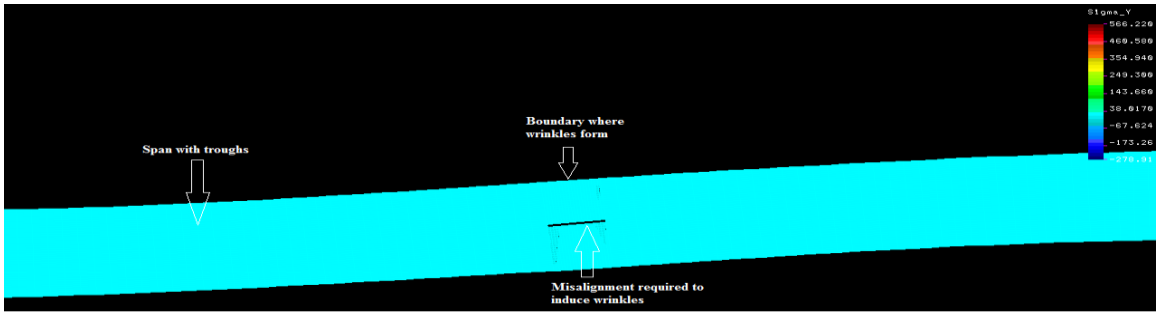

Figure 14 - Deformed Model showing σ_y Stress Output

The output of the compressive principal stress across a non-uniform web approaching a misaligned roller is shown in Figure 15.

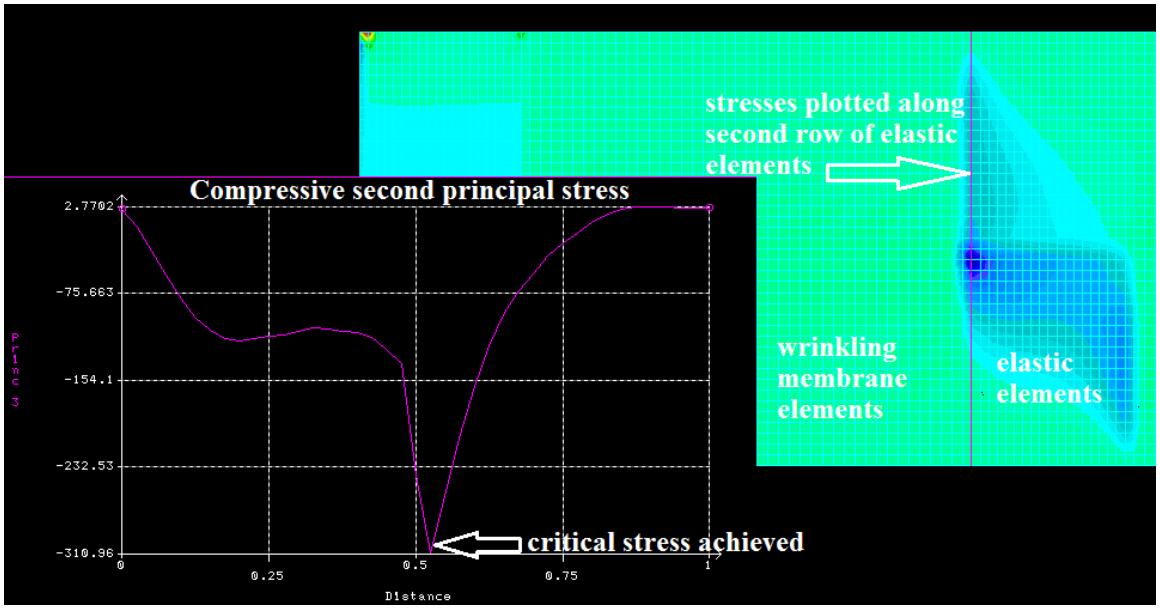

Figure 15 - Critical σ_2 Stress developed in FE analysis of the Misaligned Roller

4.4 Troughs Due to Misaligned Roller

The linear analysis of the model described for wrinkles gives the critical misalignment required for the onset of troughs. The linear analysis was carried out by varying different parameters like the web line tension and aspect ratio. This type of analysis does not take into account the time curves. The σ_x stresses and shear forces both applied directly in a single step. After execution of model σ_2 stresses were reviewed in the middle of a free web span. When these stresses reach the critical value given by expression {1}, troughs are said to be formed. Once this critical principal stress was

attained the misalignment required for the onset of troughs can be calculated using same approach as explained earlier. The results from a linear analysis were compared with the analytical model developed.

4.5 Saint Venant's Principle

In the FE models developed it can be seen that the applied shear forces are far away from the vicinity where wrinkling was studied, look at Figure 8 and 12. The loads are applied at the roller boundaries and we are interested in stress output in the middle of the span. Hence according to St. Venant's principle [23] we can use any arrangement of these shear forces as long as the resultant forces are identical. This principle state that if an actual distribution of forces is replaced by a statically equivalent system, the distribution of stress and strain throughout the body is altered only near the regions of load application. This principle was verified for FE models by considering different load distributions for applied shear forces as shown in Figure 16, while keeping the equivalent loading constant. The three cases studied were:

1. Uniform Loading
2. Parabolic Loading
3. Step Loading

The FE model was executed three times with different types of loadings keeping equivalent shear force constant. After the execution stress and deformation outputs were

reviewed. It was observed that if we have all other parameters constant change in type of loading does not affect the resultant stresses and strains. The sample input is shown in Figure 16 where the resultant shear force is 0.796 lbs.

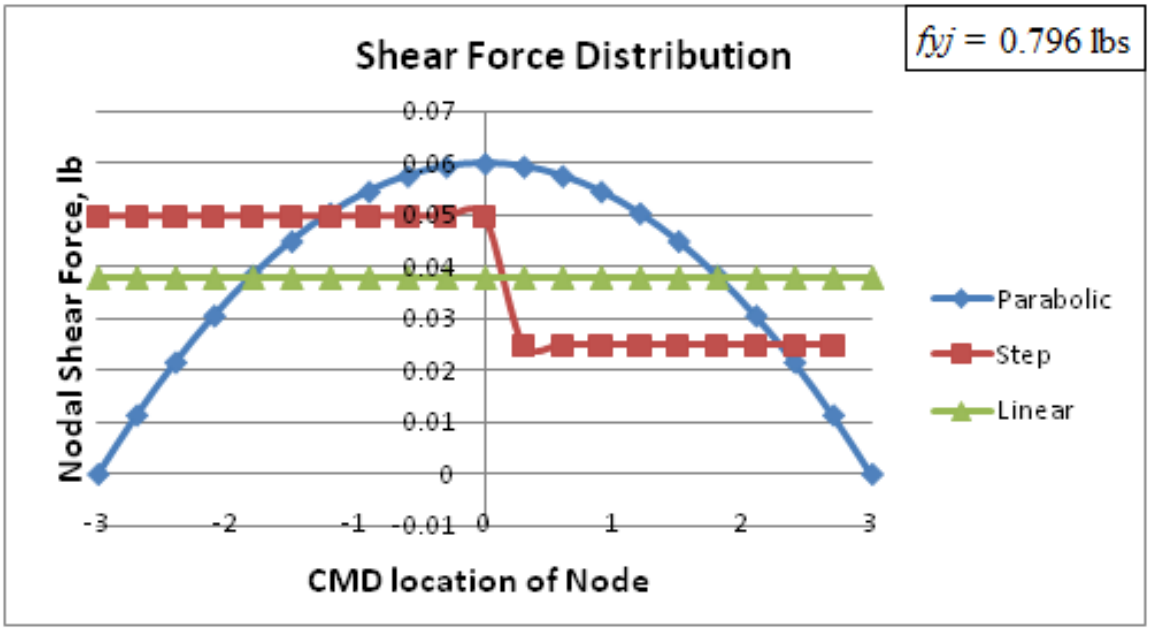

Figure 16 - Shear Force Distribution

CHAPTER V

Comparison of Results

The analytical model developed in Chapter III was compared with the results from the execution of the FE model developed in COSMOS. The model was executed for the web width of 6", the uniform web of thickness 0.001" with Young's modulus of 725000 psi and Poisson's ratio of 0.3. These properties are typical for bi-axially oriented polyester film. The roller radii were 1.4323" for both the upstream and downstream rollers for the tapered roller case, and 1.499" for the misaligned roller case. The cases were run for different aspect ratios which is the ratio of the span length to the width of the web (a/b = 1-5) and different web line tensions (5-40 lbs). The non-uniform web was modeled with the thickness on the thinner side of web= 0.001" and the thickness on the thicker side of web= 0.002".

5.1 Results for a Tapered Roller

Figure 17 replicates the comparison of analytically determined values from Beisel's approach [15] for a critical taper at a given aspect ratio to the FE models for the uniform web with 0.001" thickness, non-uniform web (h_1=0.001", h_2=0.002") and the web line tension T=16.56 lbs. The FE model was acceptable in predicting the onset of troughs in a web span due to a tapered roller for a range of aspect ratio. The procedure for using linear finite element analysis to predict troughs was presented in Chapter IV, Page 45. For the analytical model for a non-uniform web a factor of k=2.18 from expression {27} was used for calculating the maximum shear stress which was then used to calculate the critical taper using expression {28}. As the aspect ratio increases additional taper is required to generate a trough. At low aspect ratio (a/b=1) the theory was unable to give good results predominantly due to the shear effects. The results presented here correlates well with the experimental data generated by Beisel for a polyester web of 0.00092" thickness (for instance a/b = 5, taper required to induce a trough in the web was 0.00063 in/in). It requires more taper to generate a trough in the uniform web encountering a tapered roller than the non-uniform web. This is because more shear is produced in the non-uniform web for a given taper since it has greater area moment of inertia.

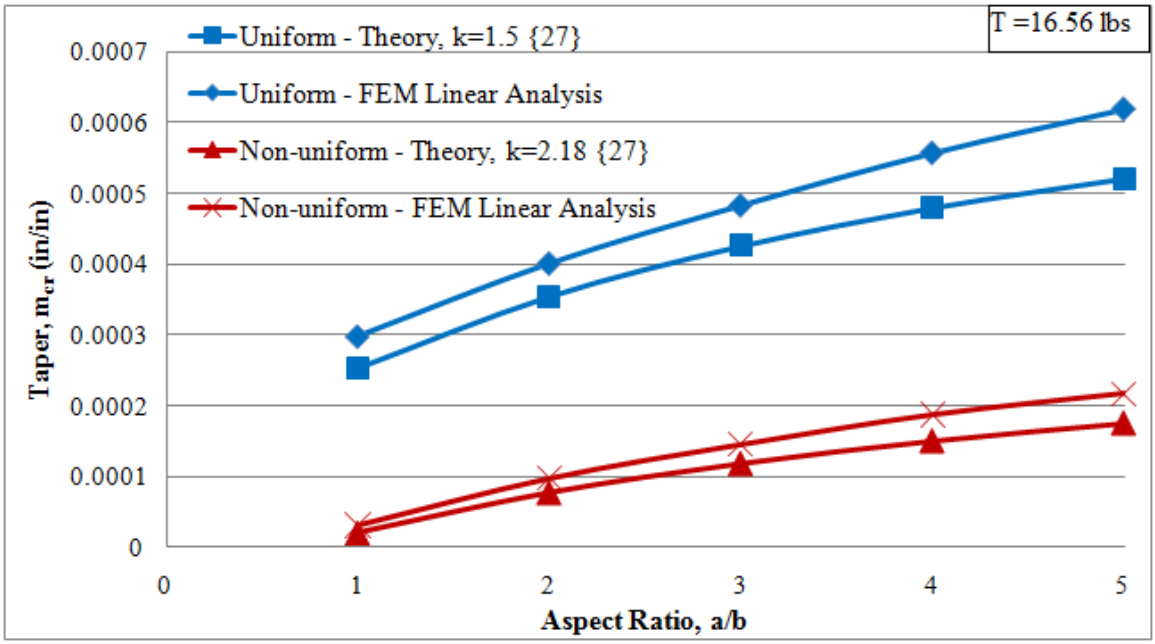

Figure 17 - Troughs Due to Taper-Aspect Ratio

In Figure 18 it can be seen that if we run FE models using a non-linear analysis the post buckling analysis gives us the critical taper values for the onset of wrinkling. In this analysis the Miller-Hedgepeth elements described in Chapter II are used in the free spans. If tension is kept constant (T=16.56 lbs) as we go on increasing the aspect ratio it will require more taper to induce a wrinkle in the web. Also for the same aspect ratio the uniform web can withstand more taper than the non-uniform web before a wrinkle forms. The maximum compressive stresses that initiate buckling appear in the middle of the web width approaching a tapered roller in case of the uniform web, while for the non-uniform web the maximum compressive stresses first appear in the thinner side of web.

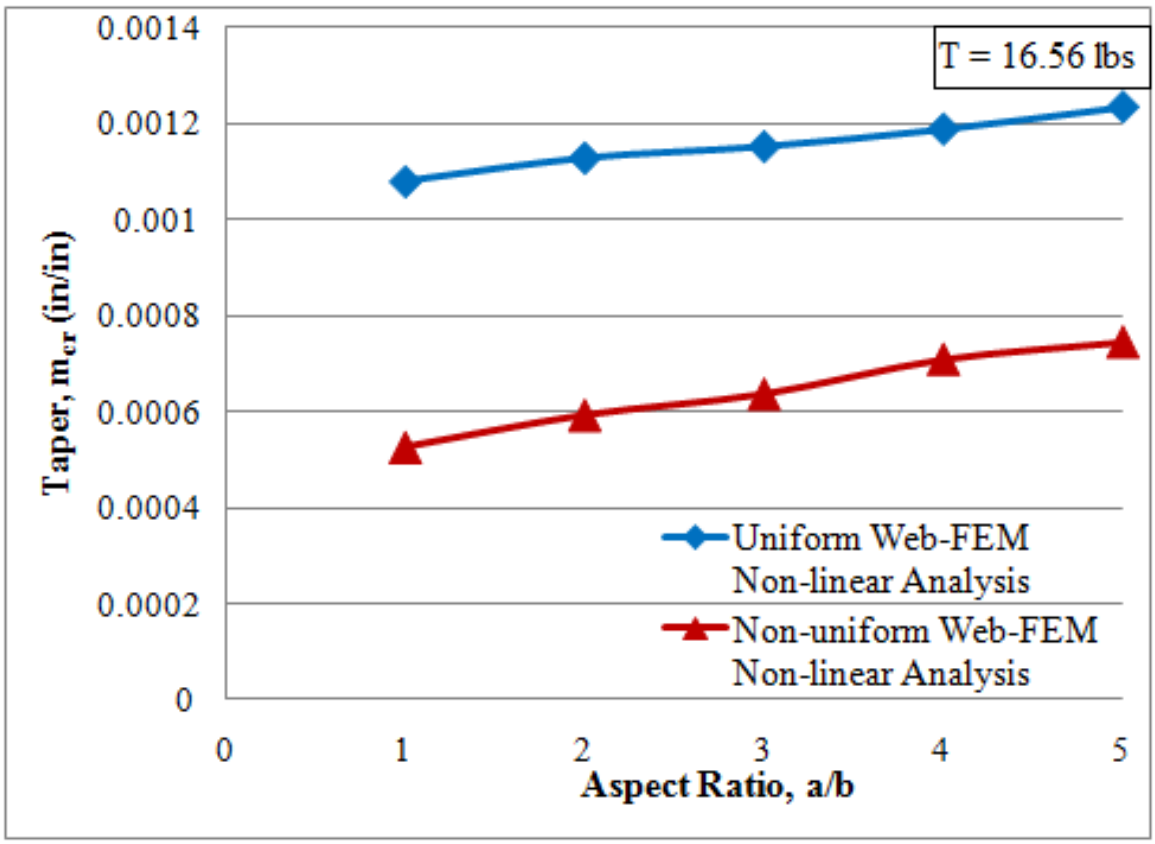

Figure 18 - Wrinkles Due to Taper-Aspect Ratio

Now the aspect ratio is kept constant (a/b=5; Span length a=30”, Web width b=6”) and the web line tension was increased step by step from 0 to 40 lbs. The Figure 19 shows the comparison of analytical values for a critical taper with the FE model results. The graph shows FE results in good agreement with analytical values for low tension levels. There is slight variation between results for higher web line tensions. For the analytical model of non-uniform web a factor of k=2.18 from expression {27} was used for calculating the maximum shear stress which was then used to calculate the critical taper using expression {28}. The linear analysis of the FE model shows that the uniform web is more stable than the non-uniform web. It requires more taper to generate a taper in

the uniform web encountering a tapered roller than the non-uniform web for the same web line tension. This is because more shear is produced in the non-uniform web for a given taper since it has greater area moment of inertia.

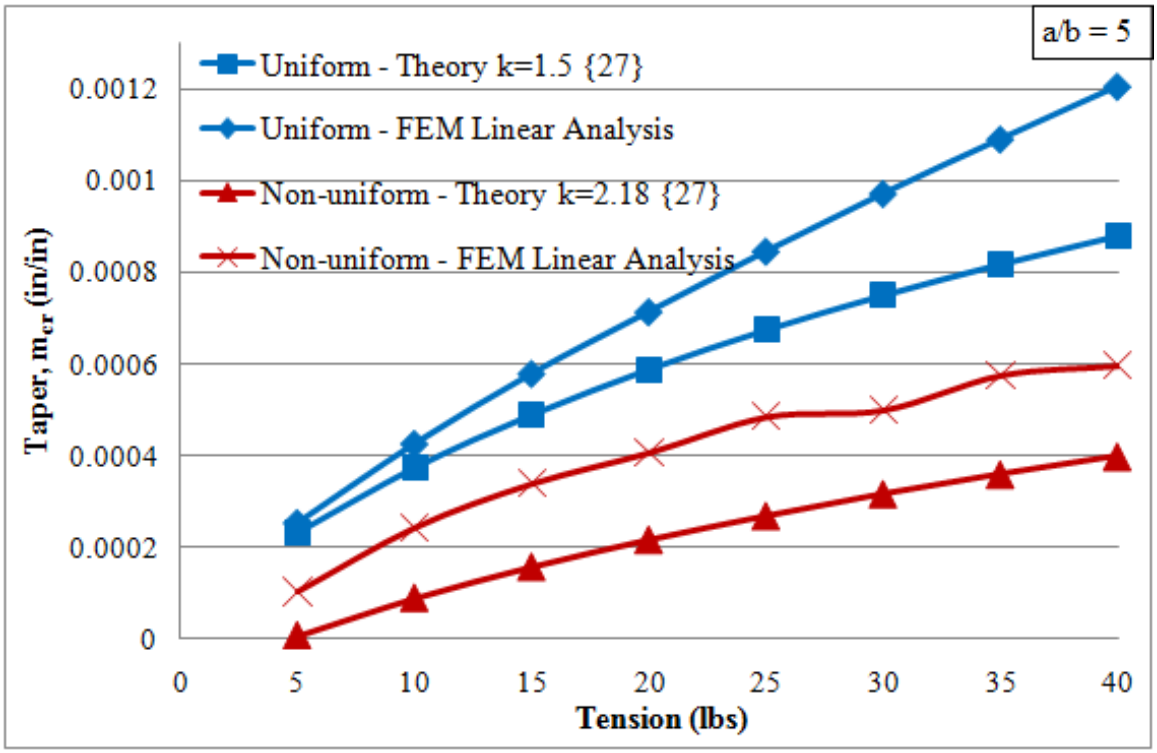

Figure 19 - Troughs Due to Taper-Varying Tension

In Figure 20 it can be seen that if we run FE models using a non-linear analysis, the post buckling analysis gives us the critical taper values for the onset of wrinkling. In this analysis the Miller-Hedgepeth elements described in Chapter II are used in the free spans. If the aspect ratio is kept constant (a/b=5) as we go on increasing the web line tension it will require more taper to induce a wrinkle in the web. Also for the same web line tension the uniform web can withstand more taper than the non-uniform web before a wrinkle forms. In the non-uniform web the maximum compressive stress that initiate

buckling first appear in the thinner side of the web. For lower tension values (T<5 lbs) the model does not produce result as the slack edge forms as per expression {49} before the critical stress for wrinkling given by expression {2 } is reached.

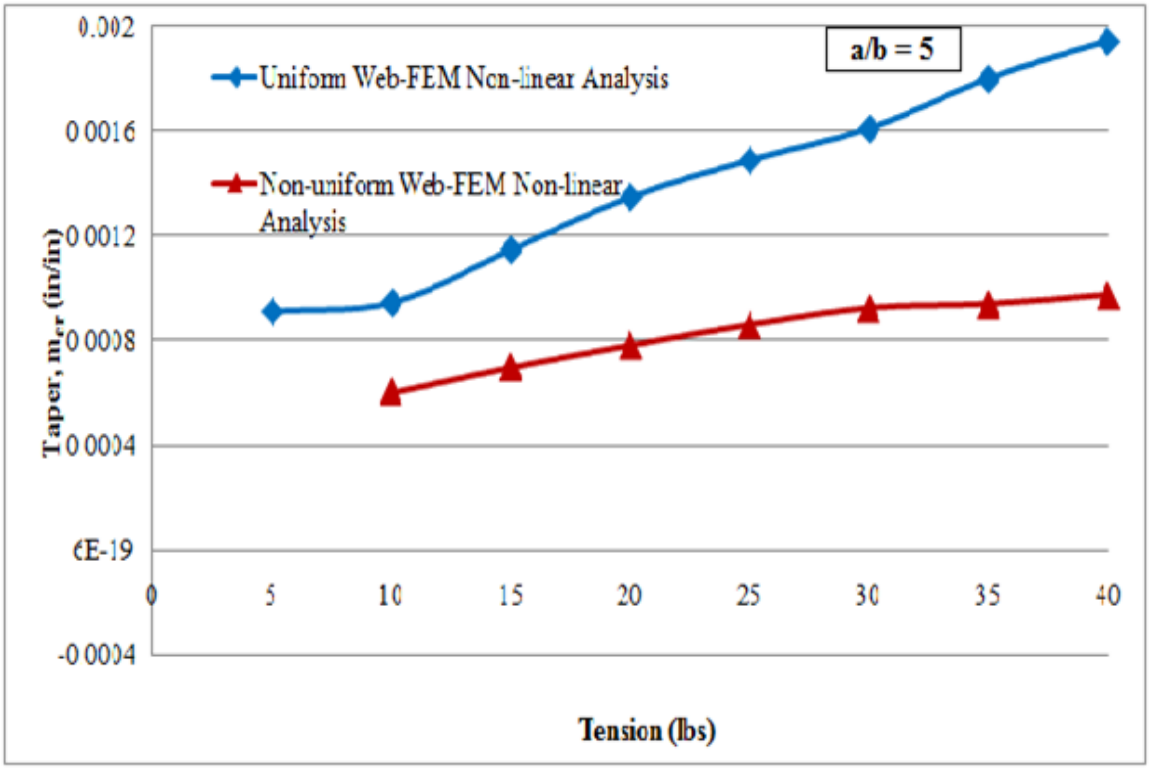

Figure 20 - Wrinkles Due to Taper-Varying Tension

In case of non-uniform web case presented herein the thicker side of the web can be either on left or right side. Both the cases were studied over a range of aspect ratio. The change in orientation was responsible for shifting the centroidal axis of the web cross-section. Also the relative velocity of the web was changed with respect to CMD location, which was responsible for generation of moment in opposite direction at the downstream roller. The models produced different values for the critical taper required to

induce troughs depending on the orientation of the web cross-section on to a tapered roller as shown in Figure 21.

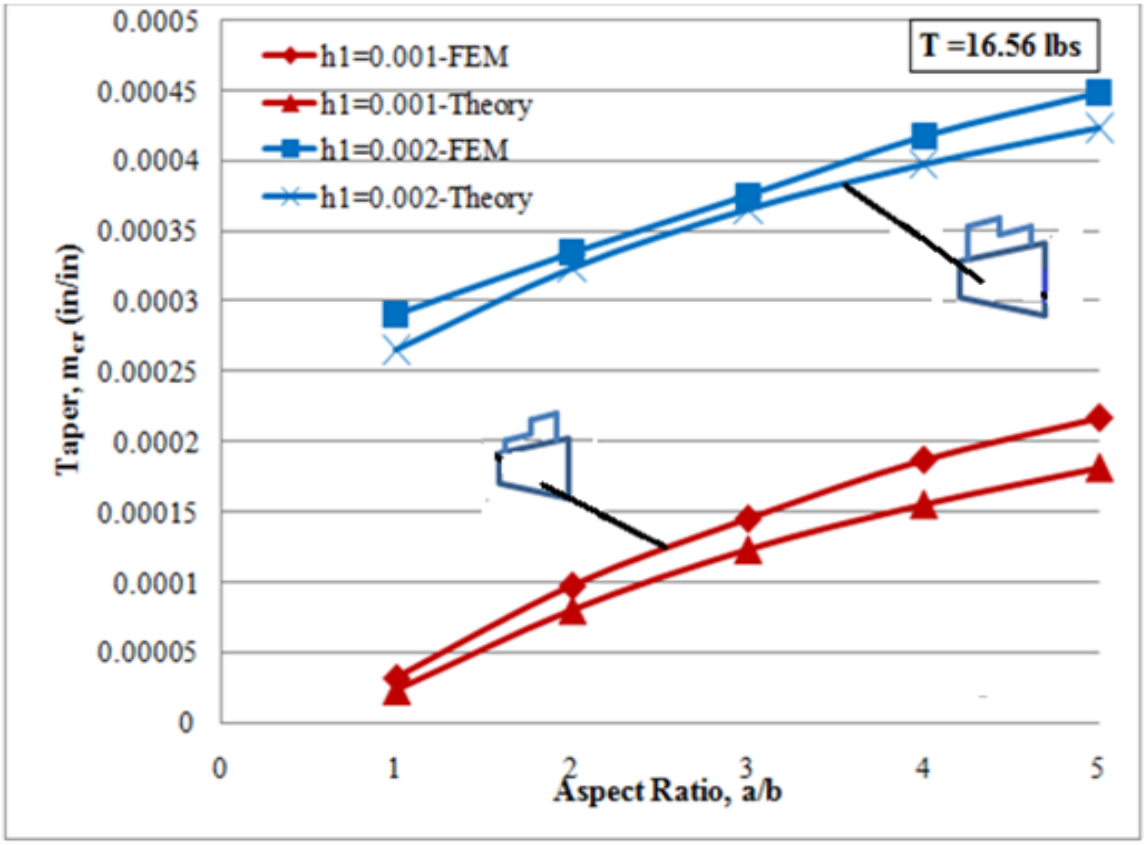

Figure 21 - Effect of Orientation of Web on a Tapered Roller

Figure 22 shows the results for critical taper required for the onset of troughs for three different cases. It can be seen that uniform web is more stable than non-uniform webs considered herein. The difference in degree of taper required for the onset of troughs arises due to changing moment of inertia of web cross-section. Also, in case of non-uniform web with the thinner side of 0.0005" the critical buckling stress given by expression {1} will be lower than other two cases, which also affects the taper required to induce troughs.

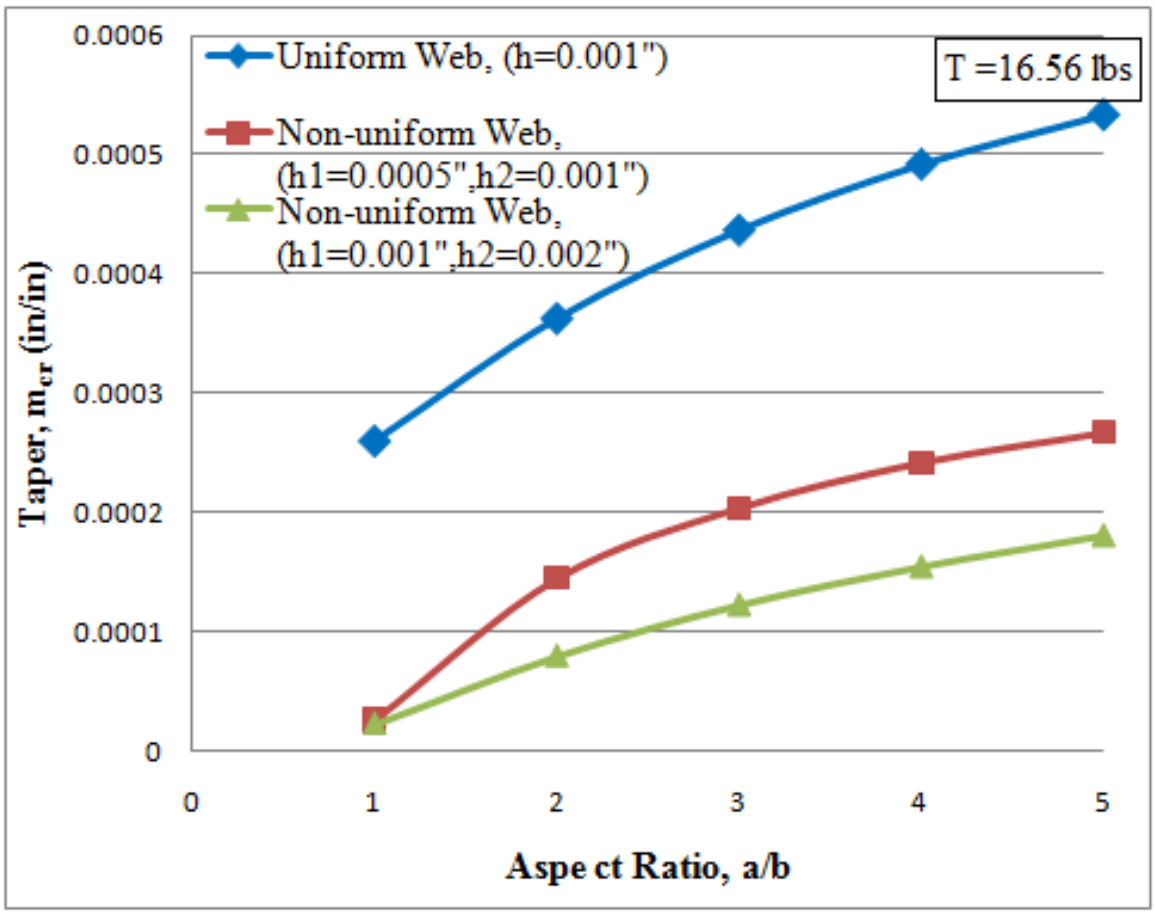

Figure 22 - Effect of Variation in thickness parameter

5.2 Results for a Misaligned Roller

Figure 23 shows the comparison of analytically determined values from Beisel's approach [15] for a critical misalignment at a given aspect ratio to FE models for the uniform web with 0.001" thickness and web line tension T=16.56 lbs. In the analytical model the factor k=1 is used instead of k=1.5, expression {27}, for the maximum shear stress calculation. Beisel observed that factor k=1 gives good approximation when comparing analytically determined values with the experimental and FE results. These

results verify this behavior too. The FE model was showing good agreement with the analytical model in predicting the onset of trough in a web span due to a misaligned roller. For the analytical model of non-uniform web the factor of k=2.18, from expression {27}, instead of k=1 was used for calculating the maximum shear stress which was then used to calculate the critical misalignment using expression {39}. As the aspect ratio increases additional misalignment is required to generate a trough. For the same aspect ratio the uniform web can withstand more misalignment than the non-uniform web before trough formation. This is because more shear is produced in the non-uniform web for a given misalignment since it has greater area moment of inertia.

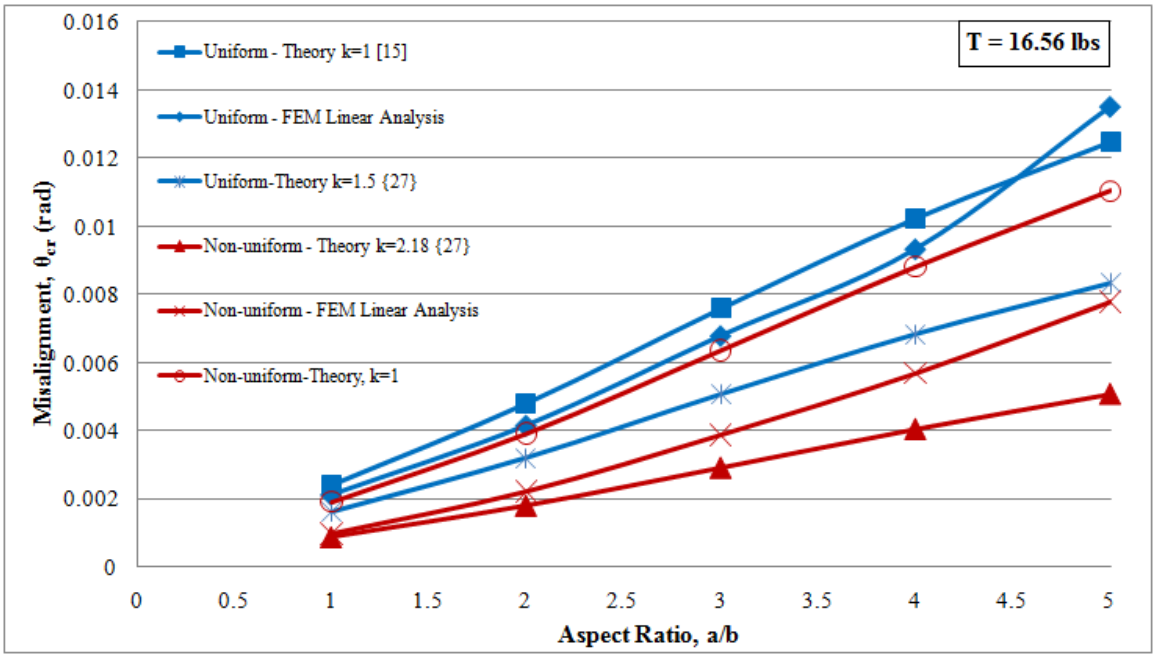

Figure 23 - Troughs Due to Misalignment-Aspect Ratio

In Figure 24 it can be seen that if we run FE models using a non-linear analysis, the post buckling analysis gives us the critical misalignment values for the onset of

wrinkling. If the tension is kept constant (T=25 lbs) as we go on increasing the aspect ratio it will require more misalignment to induce a wrinkle in the web. Also for the same aspect ratio the uniform web can withstand more misalignment than the non-uniform web considered herein before a wrinkle forms. This is because more shear is produced in the non-uniform web for a given misalignment since it has greater area moment of inertia.

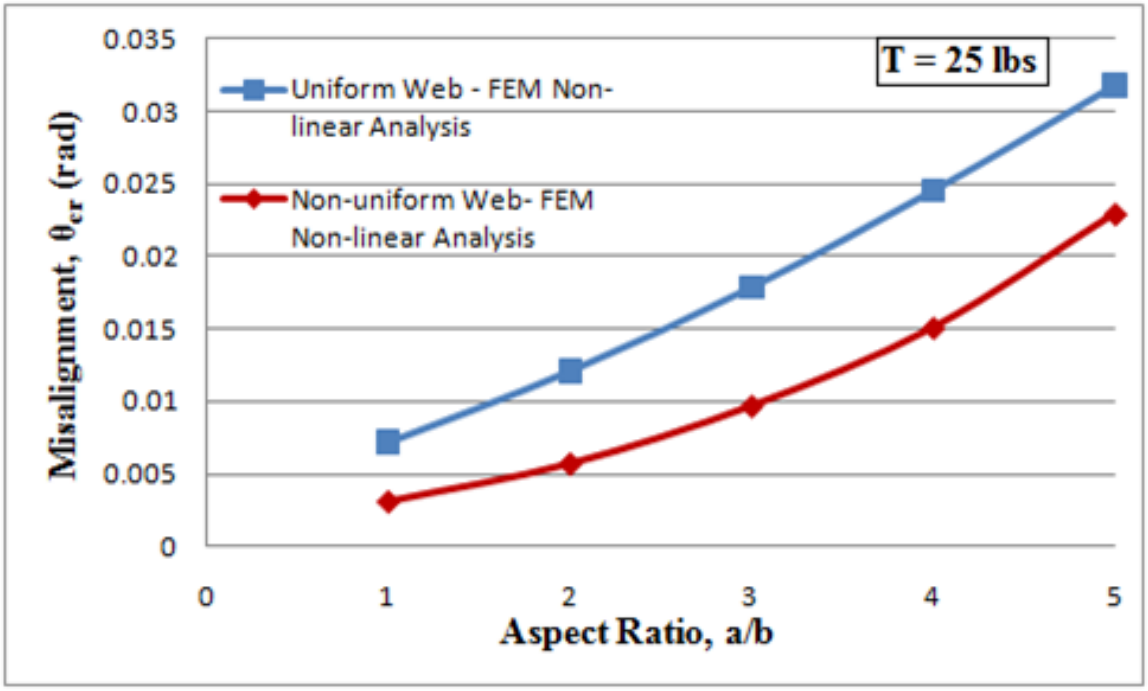

Figure 24 - Wrinkles Due to Misalignment-Aspect Ratio

Figure 25 shows the comparison of analytically determined values from Beisel's approach [15] for a critical misalignment at a given web line tension to FE models for the uniform web with 0.001" thickness, non-uniform web (h_1=0.001", h_2=0.002") and a web span of a=18". Beisel used the factor k=1 for the shear stress calculation in the analytical model based on his observations in experimental results. For the analytical model of non-uniform web a factor of k=2.18, from expression {27}, instead of k=1 was used for

calculating the maximum shear stress which was then used to calculate the critical misalignment using expression {39}. The procedure for using linear finite element analysis to predict troughs was presented in Chapter IV, Page49. The FE model was showing good agreement with the analytical model in predicting the onset of troughs in a web span due to a misaligned roller at lower aspect ratio. But for long spans the theory developed was not able to produce good approximation. As we can see the uniform web is more stable than the non-uniform web. It requires more misalignment to generate a trough in the uniform web encountering a misaligned roller than the non-uniform web. This is because more shear is produced in the non-uniform web for a given misalignment since it has greater area moment of inertia.

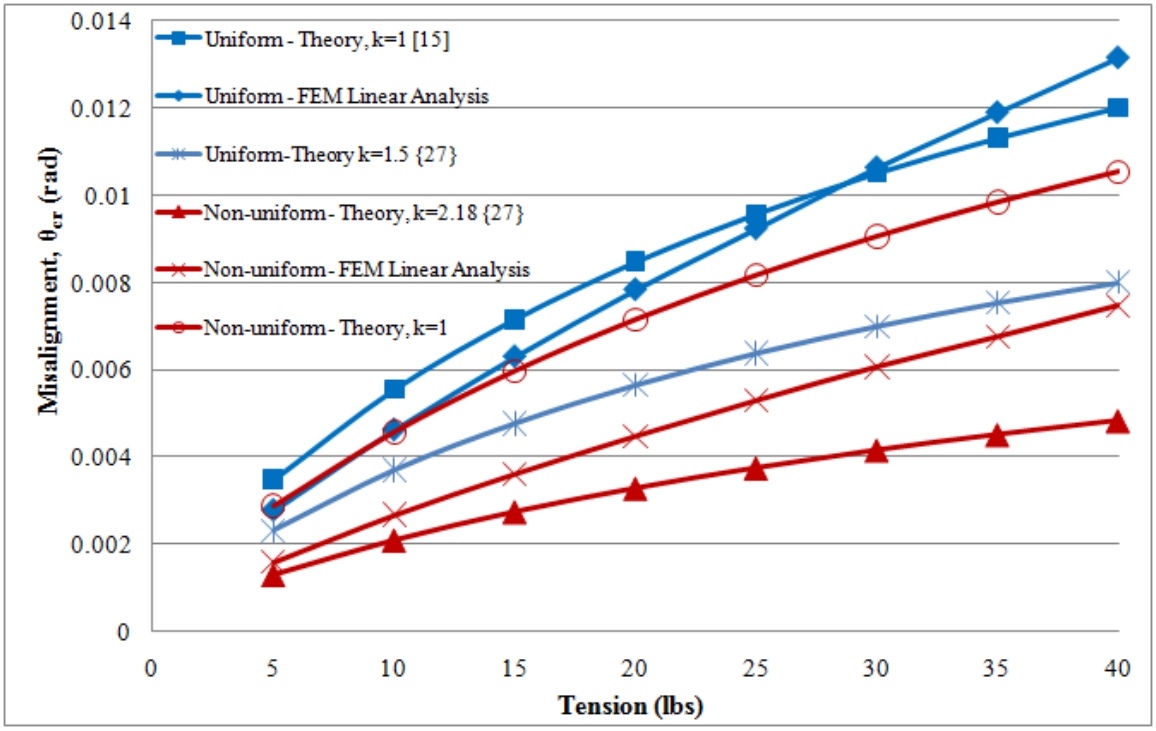

Figure 25 - Troughs Due to Misalignment-Varying Tension

The non-linear analysis of proposed wrinkling model for misaligned roller case gives us the critical misalignment values for the onset of wrinkling. If tension in the MD is increased it will require more misalignment to induce a wrinkle in the web as shown in Figure 26. Also for the same web line tension the uniform web can handle more misalignment than the non-uniform web before a wrinkle forms. For lower tension values (T<10 lbs) the model does not produce result as the slack edge forms as per expression {46} before the critical stress for wrinkling given by expression {2 } is reached.

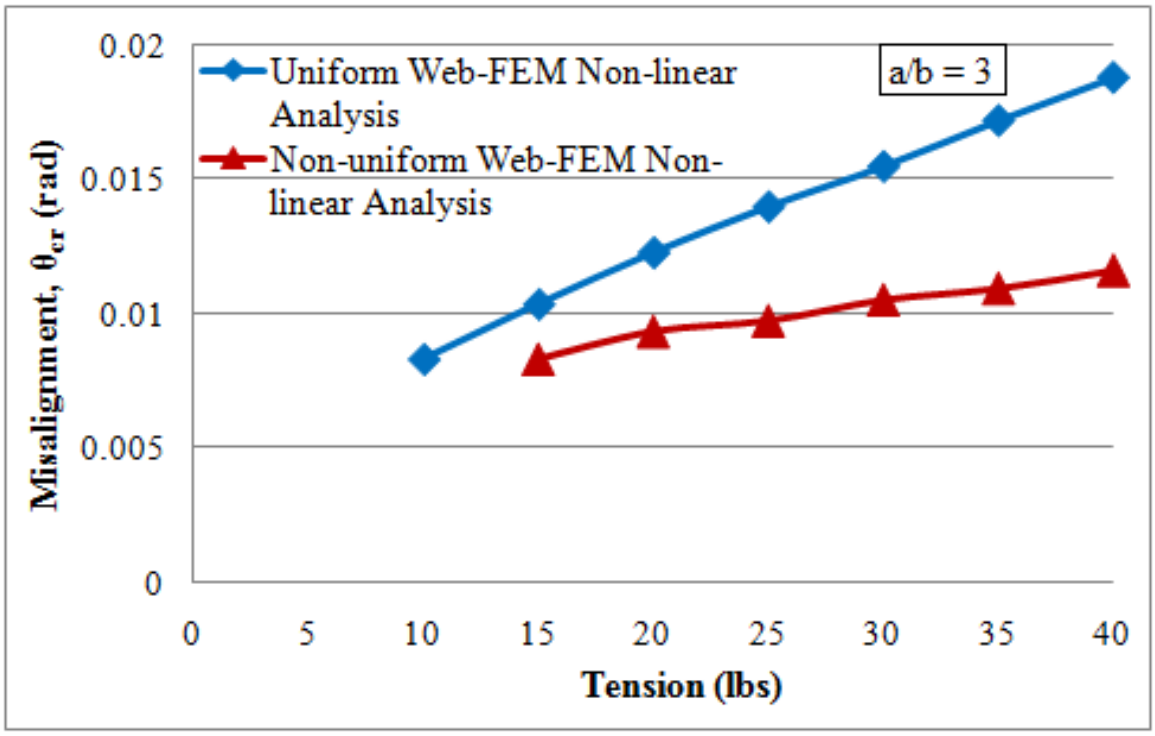

Figure 26 - Wrinkles Due to Misalignment-Varying Tension

CHAPTER VI

Conclusions and Future Work

6.1 Conclusions

1. **Linear FEA was more accurate than the closed form expression in predicting the onset of troughs in the non-uniform webs approaching tapered or misaligned rollers. (Judgment of 'k' is not required). These closed form solutions still have value for web line engineers who lack the ability or time to employ FEA. The closed form solutions typically yield conservative results that can safely be used by design engineers.**

The closed form solution was developed to predict the trough formation in non-uniform web approaching a downstream tapered roller with consideration of shear effects, tension effects and orthotropic web properties. This method is consistent with the case of a non-uniform web approaching a misaligned roller. Both these cases are presented in Chapter III. The onset of troughs can be predicted using linear analysis of FE models and the results were more accurate as compared to theoretical values derived from the closed form solution, as shown in Figures 17, 19, 23 and 25, for the critical taper and misalignment given by expressions {28} and {39} respectively.

2. **Non-linear FEA can predict the onset of wrinkles in uniform and non-uniform webs approaching tapered or misaligned rollers.**

The wrinkling of non-uniform webs while moving over a roller is modeled using wrinkling membrane elements in a FE non-linear analysis. The classical shell buckling criteria is used to calculate the critical stress for the onset of wrinkling. The cases of both the tapered and the misaligned roller are modeled using a consistent method in Chapter IV. The results for a critical taper or misalignment required for the onset of wrinkling are as shown in Figures 18, 20, 24 and 26.

3. **It has been shown herein that the non-uniform web studied is more unstable than the uniform web, the non-uniform web is more susceptible to troughs and wrinkles.**

Troughs will induce in thinner part of non-uniform web for which critical compressive stress is low. The non-uniform webs require less taper to induce troughs and wrinkles when compared to uniform webs approaching a tapered roller for same aspect ratio and tension as shown in Figures 17, 18, 19 and 20. The non-uniform webs require less misalignment to induce troughs and wrinkles when compared to uniform webs for same aspect ratio and tension as shown in Figures 23, 24, 25 and 26. Increasing aspect ratio gives more tolerance for misalignment before trough formation for both uniform and non-uniform webs as shown in Figures 23.

6.2 Future Work

The work presented here is based on assumption that as the web exits the upstream roller no slippage is allowed until the web leaves the roller. Thus this research does not take into account web traction. These traction effects may be incorporated in future modeling efforts.

The efforts can be made to model the current problems presented herein using explicit 3D CAD modeling. The problem can be modeled in software like ABAQUS with minimal boundary conditions and assumptions. The factor k=1 used in closed form solution for a critical misalignment in case of the uniform web produces good results, but still theory behind using it is not clear. If compressive stress required for buckling is evaluated over width of at least one wavelength of trough better criterion can be formulated than maximum or average shear stress criterion used in a closed form expression.

References

1. Shelton, J.J., "Lateral Dynamics of a Moving Web", PhD. Thesis, Oklahoma State University, 1968.

2. Miller, R.K. and Hedgepeth, J.M., "An Algorithm for Finite Element Analysis of Partly Wrinkled Membranes", AIAA Journal, p. 1761-1763, Dec. 1982.

3. Friedrich, C.R. and Good, J. K., "Stability sensitivity of web wrinkles on rollers", TAPPI Journal, pp. 161-165, Feb. 1989.

4. Gehlbach, L.S., Good, J.K., and Kedl, D.M., "Prediction of Shear Wrinkles in WEB Spans", TAPPI Journal, Vol. 72, No. 8, p. 129-134, Aug. 1989.

5. Gopal, H. and Kedl, D.M., "Using Finite Element Method to Define How Wrinkles Form in a Single Web Span Without Moment Transfer", Proceedings of the First International Conference on Web Handling, Stillwater, OK, WHRC, Oklahoma State University, 1991

6. Papandreadis, A., "The Development of Finite Element Modeling Techniques of Webs and the Analysis of Web Wrinkle Formation", M.S. Thesis, Oklahoma State University, July 1984.

7. Shelton, J.J., "Buckling of Webs from Lateral Compressive Forces", Proceedings of the Second International Conference on Web Handling, Stillwater, OK, WHRC, Oklahoma State University, June 1993.

8. Bensen, R.C., et al., "Simulation of Wrinkling Patterns in Webs Due to Non-Uniform Transport Conditions", Proceedings of the Second International Conference on Web Handling, Stillwater, OK, WHRC, Oklahoma State University, June 1993.

9. Good, J.K., "Shear in Multispan Web Systems", Proceedings of the Fourth International Conference on Web Handling, Stillwater, OK, WHRC, Oklahoma State University, June 1997.

10. Good, J.K., Kedl, D.M., and Shelton, J.J., "Shear Wrinkling in Isolated Spans", Proceedings of the Fourth International Conference on Web Handling, Stillwater, OK, WHRC, Oklahoma State University, June 1997.

11. Good, J.K. and Straughan, P., "Wrinkling of Webs Due to Twist", Proceedings of the Fifth International Conference on Web Handling, Stillwater, OK, WHRC, Oklahoma State University, June 1999.

12. Webb, D.K., "Prediction of Web Wrinkles Due to Misalignment of a Downstream Roll in a Web Span", M.S. Thesis, Oklahoma State University, December 2004.

13. Hashimoto, H., "Prediction Model of Paper-Web Wrinkling and Some Numerical Calculation Examples with Experimental Verifications", Proceedings of the Eighth International Conference on Web Handling, Stillwater, OK, WHRC, Oklahoma State University, June 2005.

14. Brown, J.L., "A New Method for Analyzing the Deformation and Lateral Translation of a Moving Web", Proceedings of the Eighth International Conference on Web Handling, Stillwater, OK, WHRC, Oklahoma State University, June 2005.

15. Beisel, J.A., "Single Span Web Buckling due to Roller Imperfections in the Web Process Machinery", PhD Thesis, Oklahoma State University, December 2006.

16. Mallya, Sandesh, "Investigation of the Effects of Voids on the Stability of Webs", M.S. Thesis, Oklahoma State University, December 2007.

17. Kara, Ihsan, "Wrinkle Formation due to Non-uniform length across the Width of a Web", M.S. Thesis, Oklahoma State University, July 2008.

18. Good, J.K., Beisel, J.A., Yurtcu, H, "Predicting Web Wrinkles on Rollers", Proceedings of the Tenth International Conference on Web Handling, Stillwater, OK, WHRC, Oklahoma State University, June 2009.

19. Good, J.K. and Beisel, J.A., "Buckling of Orthotropic Webs in Process Machinery", Proceedings of the Seventh International Conference on Web Handling, Stillwater, OK, WHRC, Oklahoma State University, June 2003.

20. Przemieniecki, J.S., Theory of Matrix Structural Analysis, McGraw-Hill, New York, 1968.

21. Timoshenko, S.P. and Gere, J.M., Theory of Elastic Stability, 1st ed, McGraw-Hill, New York, 1936.

22. Timoshenko, S.P. and Goodier, J.N., Theory of Elasticity, 3rd ed, McGraw-Hill, New York, 1987.

23. Ugural, A.C. and Fenster, S.K., Advanced Strength and Applied Elasticity, 3rd ed, Prentice-Hall PTR, New Jersey, 1995.

24. Lekhnitskii, S.G., Anisotropic Plates, Gordon and Breech, New York, 1968

Appendix A

The FE package used for modeling the problem was COSMOS 2.8. To start modeling first a new file is created in COSMOS. That would give a blank screen with coordinate axis system. To create the geometry proper plane was then selected using VIEW command. Then model geometry was created using points, curves and surfaces. Next, the element group 1 for elastic portion of the web was selected. This element group utilized the Shell4 element in COSMOS. This element is 4 node quadrilateral elements used to model the thin shells. In COSMOS 4 node element is made up of 4 triangles instead of a whole quadrilateral element as one unit. This element shows symmetry behavior in symmetric problems and accuracy of calculations is good. All the default settings of element group (such as regular elastic behavior and linear elastic material) were used except that large displacement formulations were selected. Then the material properties E_x and ν were entered. Next, the thickness was entered under the Real Constants. Once the elastic element groups were defined in geometry the second element group was defined. This element group was used to model the web with developed troughs. Again the Shell4 elements were selected, but now the membrane analysis was selected instead of regular analysis. Next, wrinkling membrane input was selected in the

material type; all other default settings were maintained for this element. The wrinkling membrane elements could not withstand compression in σ_2 direction. Once the wrinkling membrane option is selected the analysis is required to be non-linear due to state dependent material properties.

The grid size was set to 40 elements across the 6" width of the web. In the web span where stresses changed slowly, the elements were set to be approximately 3 times longer than their width. In the area of rollers, on the boundary between element types where the compressive stresses were expected to develop, the length of the elements was set to ½ their width. The nodes were then merged together using NMERGE within tolerance of 0.0001 and then again renumbered automatically by COSMOS through NDUPDATE command. All the boundary conditions discussed in Chapter III were then implemented into the model through load boundary conditions option, which allows to set coupling constraints and locks degrees of freedom of nodes which are not required. The web line tension was then applied as a uniform stress σ_x across the width at both the ends of the model. The lateral load was also applied evenly on nodes as shown in Figure 8.

A non-linear analysis was required to converge at each step but if too large a time step of load increment was applied then convergence was not achieved. The total time was set to 1 with a time step of 0.05. Thus the load was applied in 20 time steps. All other default settings in COSMOS were kept unchanged. The force control technique was used

along with Newton Raphson method instead of the default Modified Newton Raphson method.

A sample session file is given below; this file was used for the simulation of wrinkle formation in case of the non-uniform web approaching a tapered roller. E=725000 psi, ν=0.3, h_1=0.001", h_2=0.002", b=6", a=30", R=1.43239". A web line tension was set at T=30 lbs by applying the pressure in the form of uniform stress σ_x =3333.33 psi. The lateral load fyj=0.43092 lbs was applied at roller boundaries as shown earlier in Figure 6. The lateral loads were multiplied by scaling factor of 1.95 through time curve 2, a value know to cause the critical CMD stress. The determination of correct scaling factor requires some iterative procedure. From equation {2} a critical compressive stress of 306.334 psi is required for the onset of wrinkle.

The session file (with extension .ses) may be loaded into COSMOS, by selecting File-Load-then selecting text file which can be created from copying and pasting the following text code into notepad or another text editor.

C* COSMOSM GeoStar 2.8 (256K Version)

C* Problem : Non-uniform web Date : 02-02-2009 Time : 14:58:05

VIEW,0,0,1,0

PT,1,0,0,0

PT,2,2.25,0,0

PT,3,31.75,0,0

PT,4,32.25,0,0

PT,5,34.5,0,0

PT,6,64.5,0,0

PT,7,66.75,0,0

PT,8,0,3,0

PT,9,2.25,3,0

PT,10,31.75,3,0

PT,11,32.25,3,0

PT,12,34.5,3,0

PT,13,64.5,3,0

PT,14,66.75,3,0

PT,15,0,6,0

PT,16,2.25,6,0

PT,17,31.75,6,0

PT,18,32.25,6,0

PT,19,34.5,6,0

PT,20,64.5,6,0

PT,21,66.75,6,0

SF4PT,1,1,2,9,8,0

SF4PT,2,2,3,10,9,0

SF4PT,3,3,4,11,10,0

SF4PT,4,4,5,12,11,0

SF4PT,5,5,6,13,12,0

SF4PT,6,6,7,14,13,0

SF4PT,7,8,9,16,15,0

SF4PT,8,9,10,17,16,0

SF4PT,9,10,11,18,17,0

SF4PT,10,11,12,19,18,0

SF4PT,11,12,13,20,19,0

SF4PT,12,13,14,21,20,0

EGROUP,1,SHELL4,2,0,0,0,0,1,0,0

MPROP,1,EX,725000

MPROP,1,NUXY,0.3

RCONST,1,1,1,7,0.001,0,0,0,0,0,1E-008

M_SF,1,1,1,4,20,20,1,1

M_SF,4,4,1,4,20,20,1,1

M_SF,6,6,1,4,20,20,1,1

EGROUP,2,SHELL4,2,1,0,0,10,1,0,0

M_SF,3,3,1,4,10,20,1,1

M_SF,2,2,1,4,40,20,1,1

ACTSET,EG,1

M_SF,5,5,1,4,40,20,1,1

EGROUP,3,SHELL4,2,0,0,0,0,1,0,0

MPROP,1,EX,725000

MPROP,1,NUXY,0.3

RCONST,2,2,1,7,0.002,0,0,0,0,0,1E-008

M_SF,7,7,1,4,20,20,1,1

M_SF,10,10,1,4,20,20,1,1

M_SF,12,12,1,4,20,20,1,1

EGROUP,4,SHELL4,2,1,0,0,10,1,0,0

M_SF,9,9,1,4,10,20,1,1

M_SF,8,8,1,4,40,20,1,1

ACTSET,EG,3

M_SF,11,11,1,4,40,20,1,1

NMERGE,1,6552,1,0.0001,0,1,0

NDUPDATE,0

DSF,1,UZ,0,12,1,RY,RX,

DND,872,UX,0,872,1,UY,

A_NONLINEAR,S,1,1,20,0.001,0,N,1,0,1E+010,0.001,0.01,0,1,0,0

CPDOFND,1,UY,1,1,21,1

CPDOFND,4,UY,22,22,42,1

CPDOFND,7,UY,43,43,63,1

CPDOFND,10,UY,64,64,84,1

CPDOFND,13,UY,85,85,105,1

CPDOFND,16,UY,106,106,126,1

CPDOFND,19,UY,127,127,147,1

CPDOFND,22,UY,148,148,168,1

CPDOFND,25,UY,169,169,189,1

CPDOFND,28,UY,190,190,210,1

CPDOFND,31,UY,211,211,231,1

CPDOFND,34,UY,232,232,252,1

CPDOFND,37,UY,253,253,273,1

CPDOFND,40,UY,274,274,294,1

CPDOFND,43,UY,295,295,315,1

CPDOFND,46,UY,316,316,336,1

CPDOFND,49,UY,337,337,357,1

CPDOFND,52,UY,358,358,378,1

CPDOFND,55,UY,379,379,399,1

CPDOFND,58,UY,400,400,420,1

CPDOFND,61,UY,421,421,441,1

CPDOFND,64,UY,3298,3298,3318,1

CPDOFND,67,UY,3319,3319,3339,1

CPDOFND,70,UY,3340,3340,3360,1

CPDOFND,73,UY,3361,3361,3381,1

CPDOFND,76,UY,3382,3382,3402,1

CPDOFND,79,UY,3403,3403,3423,1

CPDOFND,82,UY,3424,3424,3444,1

CPDOFND,85,UY,3445,3445,3465,1

CPDOFND,88,UY,3466,3466,3486,1

CPDOFND,91,UY,3487,3487,3507,1

CPDOFND,94,UY,3508,3508,3528,1

CPDOFND,97,UY,3529,3529,3549,1

CPDOFND,100,UY,3550,3550,3570,1

CPDOFND,103,UY,3571,3571,3591,1

CPDOFND,106,UY,3592,3592,3612,1

CPDOFND,109,UY,3613,3613,3633,1

CPDOFND,112,UY,3634,3634,3654,1

CPDOFND,115,UY,3655,3655,3675,1

CPDOFND,118,UY,3676,3676,3696,1

CPDOFND,121,UY,3697,3697,3717,1

CPDOFND,124,UY,883,883,903,1

CPDOFND,127,UY,904,904,924,1

CPDOFND,130,UY,925,925,945,1

CPDOFND,133,UY,946,946,966,1

CPDOFND,136,UY,967,967,987,1

CPDOFND,139,UY,988,988,1008,1

CPDOFND,142,UY,1009,1009,1029,1

CPDOFND,145,UY,1030,1030,1050,1

CPDOFND,148,UY,1051,1051,1071,1

CPDOFND,151,UY,1072,1072,1092,1

CPDOFND,154,UY,1093,1093,1113,1

CPDOFND,157,UY,1114,1114,1134,1

CPDOFND,160,UY,1135,1135,1155,1

CPDOFND,163,UY,1156,1156,1176,1

CPDOFND,166,UY,1177,1177,1197,1

CPDOFND,169,UY,1198,1198,1218,1

CPDOFND,172,UY,1219,1219,1239,1

CPDOFND,175,UY,1240,1240,1260,1

CPDOFND,178,UY,1261,1261,1281,1

CPDOFND,181,UY,1282,1282,1302,1

CPDOFND,184,UY,1303,1303,1323,1

CPDOFND,187,UY,4180,4180,4200,1

CPDOFND,190,UY,4201,4201,4221,1

CPDOFND,193,UY,4222,4222,4242,1

CPDOFND,196,UY,4243,4243,4263,1

CPDOFND,199,UY,4264,4264,4284,1

CPDOFND,202,UY,4285,4285,4305,1

CPDOFND,205,UY,4306,4306,4326,1

CPDOFND,208,UY,4327,4327,4347,1

CPDOFND,211,UY,4348,4348,4368,1

CPDOFND,214,UY,4369,4369,4389,1

CPDOFND,217,UY,4390,4390,4410,1

CPDOFND,220,UY,4411,4411,4431,1

CPDOFND,223,UY,4432,4432,4452,1

CPDOFND,226,UY,4453,4453,4473,1

CPDOFND,229,UY,4474,4474,4494,1

CPDOFND,232,UY,4495,4495,4515,1

CPDOFND,235,UY,4516,4516,4536,1

CPDOFND,238,UY,4537,4537,4557,1

CPDOFND,241,UY,4558,4558,4578,1

CPDOFND,244,UY,4579,4579,4599,1

CPDOF,247,UX,9,21,42,63,84,105,126,147,168,189

CPDOF,248,UX,9,21,210,231,252,273,294,315,336,357

CPDOF,249,UX,5,21,378,399,420,441

CPDOF,250,UX,9,21,3318,3339,3360,3381,3402,3423,3444,3465

CPDOF,251,UX,9,21,3486,3507,3528,3549,3570,3591,3612,3633

CPDOF,252,UX,5,21,3654,3675,3696,3717

CPDOF,253,UY,2,442,1333

CPDOF,254,UY,2,463,1344

CPDOF,255,UY,2,484,1355

CPDOF,256,UY,2,505,1366

CPDOF,257,UY,2,526,1377

CPDOF,258,UY,2,547,1388

CPDOF,259,UY,2,568,1399

CPDOF,260,UY,2,589,1410

CPDOF,261,UY,2,610,1421

CPDOF,262,UY,2,631,1432

CPDOF,263,UY,2,652,1443

CPDOF,264,UY,2,673,1454

CPDOF,265,UY,2,694,1465

CPDOF,266,UY,2,715,1476

CPDOF,267,UY,2,736,1487

CPDOF,268,UY,2,757,1498

CPDOF,269,UY,2,778,1509

CPDOF,270,UY,2,799,1520

CPDOF,271,UY,2,820,1531

CPDOF,272,UY,2,841,1542

CPDOF,273,UY,2,862,1553

CPDOF,274,UY,2,3739,4620

CPDOF,275,UY,2,3760,4631

CPDOF,276,UY,2,3781,4642

CPDOF,277,UY,2,3802,4653

CPDOF,278,UY,2,3823,4664

CPDOF,279,UY,2,3844,4675

CPDOF,280,UY,2,3865,4686

CPDOF,281,UY,2,3886,4697

CPDOF,282,UY,2,3907,4708

CPDOF,283,UY,2,3928,4719

CPDOF,284,UY,2,3949,4730

CPDOF,285,UY,2,3970,4741

CPDOF,286,UY,2,3991,4752

CPDOF,287,UY,2,4012,4763

CPDOF,288,UY,2,4033,4774

CPDOF,289,UY,2,4054,4785

CPDOF,290,UY,2,4075,4796

CPDOF,291,UY,2,4096,4807

CPDOF,292,UY,2,4117,4818

CPDOF,293,UY,2,4138,4829

CURDEF,TIME,1,1,0,0,0.2,1,1,1

PCR,3,-3333.33,21,18,-3333.33,4

PCR,19,-3333.33,32,13,-3333.33,4

CURDEF,TIME,2,1,0,0,0.2,0,1,1.95

FND,42,FY,-0.00567,3696,3654

FND,63,FY,-0.01134,441,21

FND,3318,FY,-0.01134,3675,21

FND,904,FY,-0.00567,4558,3654

FND,925,FY,-0.01134,1303,21

FND,4180,FY,-0.01134,4537,21

FND,463,FY,0.00567,4117,3654

FND,484,FY,0.01134,862,21

FND,3739,FY,0.01134,4096,21

FND,483,FY,0.00567,4137,3654

FND,504,FY,0.01134,882,21

FND,3759,FY,0.01134,4116,21

TIMES,0,1,0.05

NL_CONTROL,0,1.

VITA

Amol Mahadev Patil

Candidate for the Degree of

Master of Science

Thesis TROUGH AND WRINKLING ANALYSIS OF NON-UNIFORM WEBS

Major Field: Mechanical and Aerospace Engineering

Biographical:

Personal Data: Born in Kolhapur, Maharashtra, India, on August 21, 1981, the son of Mahadev and Kamal Patil

Education:

Completed the requirements for the Master of Science in Mechanical and Aerospace Engineering at Oklahoma State University, Stillwater, Oklahoma in May, 2010; received Bachelor of Science in Automobile Engineering, from Shivaji University, Kolhapur, India, in May 2003; Graduated from Vivekanand College, Kolhapur, India in May 1999.

Experience:

Graduate Teaching and Research Assistant-Department of Mechanical Engineering at Oklahoma State University, Stillwater, 2008 to Present
Design Engineer, TYCO Electronics, India, 2007
Service Engineer, DSK TOYOTA, India, 2004-2006

Professional Memberships: Member of Golden Key International Honor Society

Name: Amol Mahadev Patil Date of Degree: May, 2010

Institution: Oklahoma State University Location: Stillwater, Oklahoma

Title of Study: TROUGH AND WRINKLING ANALYSIS OF NON-UNIFORM WEBS

Pages in Study: 81 Candidate for the Degree of Master of Science

Major Field: Mechanical and Aerospace Engineering

Scope and Method of Study: Depending on the final product requirements webs may have thickness non-uniformities across the web width. Some products require layers of different materials to be bonded together (i.e. laminated) to meet the desired characteristics of the final product. Also there are many limitations associated with the production of webs that prevent the web from being perfectly uniform in length and thickness. This research study focuses on how non-uniform webs differ from uniform webs in terms of instability when travelling through process machinery. Much of the research to date has focused on instabilities of uniform webs. Little is known regarding whether non-uniform webs are more or less stable than uniform webs which will be examined herein. The non-uniform web approaching tapered roller and a misaligned roller were modeled using finite element techniques in COSMOS. The results from Finite Element Analysis (FEA) models were compared with closed form solutions that were developed using a structural stiffness matrix approach.

Findings and Conclusions: Linear FEA was more accurate than the closed form expressions in predicting the onset of troughs in non-uniform webs approaching tapered or misaligned roller. These closed form solutions still have value for web line engineers who lack the ability or time to employ FEA. The closed form solutions typically yield conservative results that can safely be used by design engineers. Non-linear FEA can be used to predict the onset of wrinkles in uniform and non-uniform webs approaching tapered or misaligned rollers. It has been shown herein that the non-uniform web studied is more unstable than a similar uniform web. The non-uniform web was shown to be more susceptible to troughs and wrinkles.

ADVISER'S APPROVAL: Dr. J. K. Good